UNIVERSITÀ DEGLI STUDI DI UDINE

DOTTORATO DI RICERCA IN
TECNOLOGIE CHIMICHE ED ENERGETICHE

# THERMODYNAMIC ASPECTS OF SELECTIVE COMPLEXATION OF HEAVY METAL IONS OF ENVIRONMENTAL INTEREST: FUNDAMENTALS AND APPLICATIONS

Dott. Elena PERALTA SALVADOR

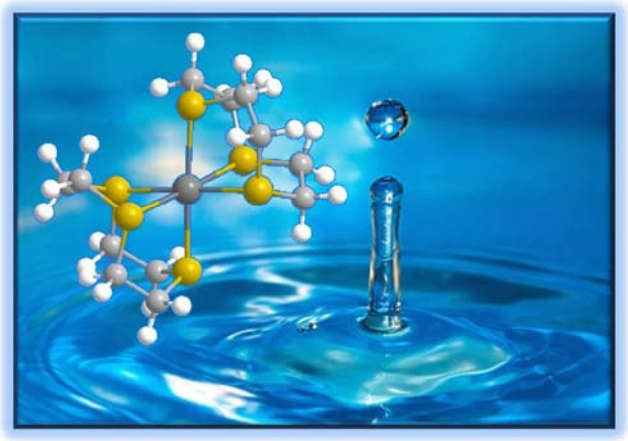

COMMISSION

| | |
|---|---|
| Prof. Josef HAVEL | REVIEWER |
| Prof. Guido CRISPONI | REVIEWER |
| Prof. Alessandro TROVARELLI | REFEREE |
| Prof. Antonino Salvatore ARICO' | REFEREE |
| Prof. Albin PINTAR | REFEREE |
| Prof. Plinio DI BERNARDO | REFEREE |
| Prof. Manuel VALIENTE | SUPERVISOR/REFEREE |
| Prof. Marilena TOLAZZI | CO-SUPERVISOR/REFEREE |
| Prof. Alfredo SOLDATI | DIRECTOR OF PH.D. PROGRAM |

# Acknowledgments

I would like to thank the persons of the Thermodynamic Group of the University of Udine: Prof. Marilena Tolazzi for her supervision and helping considerations during my PhD studies, Dr. Andrea Melchior, Dr. Davide Menotti and Dr. Pierluigi Polese for their assistance and friendly support during my time at Udine.

I would like to thank the persons from Grup de Tècniques de Separació en Química (Group of Separation Techniques in Chemistry), GTS, of the Universitat Autònoma de Barcelona (Autonomous University of Barcelona): Prof. Manuel Valiente for his guidance and support during my time at GTS and all colleagues working at GTS during last three years for their friendship and help.

I would also like to thank Prof. Claudio Tavagnacco, University of Trieste.

I also thank Friuli Venezia Giulia Region for financial support at the project "ECOMETA" which was partially carried out during this thesis.

# Table of contents

## List of abbreviations

| | |
|---|---|
| $\lambda$ | Wavelength |
| $\Delta E$ | Potential variation |
| $\Delta G^0$ | Standard Gibbs free energy |
| $\Delta H^0$ | Standard Enthalpy |
| $\Delta H_{sv}$ | Enthalpy of solvation |
| $\Delta H^{tr}$ | Enthalpy of transfer |
| $\Delta S^0$ | Standard Entropy |
| 12AneS4 | 1,4,7,10-tetrathiacyclododecane |
| 14AneS4 | 1,4,8,11-tetrathiacyclotetradecane |
| 9AneS3 | 1,4,7-trithacyclononane |
| AN | Acetonitrile |
| An(III) or $An^{3+}$ | Trivanlent actanides |
| BTPA | 6,6'-bis[bis(2-pyridylmethyl)aminimethyl]-2,2'-bipyridine |
| $C_{Ag}$ | Concentration of silver |
| CE | Counter electrode |
| $C_L$ | Concentration of ligand |
| $C_M$ | Concentration of metal |
| CS | Cellulose sponge |
| D | Distribution coefficient |
| $D_{exp}$, $D_{calc}$ | Experimental and calculated distribution coefficient, respectively |
| DFT | Density functional theory |
| $D_L$, $D_C$ | Diffusion coefficients of the free ligand and complex, respectively |
| DMF | N, N-dimethylformamide |
| DMSO | Dimethyl sulfoxide |
| $D_{ox}$, $D_{red}$ | Diffusion coefficients for Ox and Red, respectively |
| E | Cell potential |
| E(%) | Metal extraction |
| $E^0$ | Standard redox potential |

| | |
|---|---|
| $E_{1/2}$ | Half-wave potential |
| EDTA | Ethylenediaminetetraacetic acid |
| ELM | Emulsion liquid membrane |
| $Et_2S$ | Dietyl sulfide |
| $F_M$ | Formation coefficient for metal |
| FP-XRF | Field Portable X-ray Fluorescence |
| HFSLM | Hollow fiber liquid membrane |
| HSAB | Hard soft acid base theory |
| i | Electric current |
| ICP-MS | Inductively coupled plasma mass spectrometry |
| $i_L$ or $i_d$ | Limiting diffusion current |
| K or $\beta$ | Formation constant or stability constant |
| L | Ligand |
| LL | Liquid-liquid extraction |
| Ln(III) or $Ln^{3+}$ | Trivanlent lanthanides |
| M | Metal ion |
| NMR | Nuclear magnetic resonance spectroscopy |
| PS | Polyurethane sponge |
| $r^{-1}$ | Inverse of the ionic radius |
| RE | Reference electrode |
| SCE | Saturated calomel electrode |
| SLM | Solid liquid membrane |
| TEAP | Tetraethylammonium perchlorate ($NEt_4ClO_4$) |
| THAM | Tris(hydroxymethyl)aminomethane |
| TPA | Tris[(2-pyridyl)methyl]amine |
| UV-VIS | Ultraviolet–visible spectroscopy |
| WE | Working electrode |
| $\varepsilon$ | Dielectric constant |
| $\varepsilon_\lambda$ | Molar absorption coefficient |

## List of figures

## List of tables

# Abstract

Metal ion and lanthanide recognition is of fundamental importance to many areas of chemistry and biochemistry but the factors underlying the stability and selectivity of a given ligand/receptor are often not of straightforward interpretation. Recognition process may depend on a series of factors that include the nature of the donor atoms and their spatial arrangement, the backbone structure of the ligand and its rigidity, the eventual formation of chelate rings of variable size.

**Thermodynamics and extraction of heavy metal complexes with thioethers**

Metal - sulphur bond is a fundamental interaction in biochemical systems and in selective separation applications for the heavy and precious metals extraction from liquid phase. For example, numerous macrocyclic structures containing sulphur donor atoms (thiols, thioethers, thioureas…) have been employed as selective extractants in a range of solvent extraction and bulk membrane transport studies.

In this section, we present the first thermodynamic investigation concerning the complex formation by several linear and macrocyclic thioethers and the Zn(II), Cd(II), and Hg(II) ions in organic solvents, such as acetonitrile (AN) and dimethyl sulfoxide (DMSO). Our main aim is to test their potential as efficient complexing agents and selective extractants for environmentally important metal ions and rationalize the recognition process in media which present relatively low dielectric constants and are less structured than water.

*Solution thermodynamics*

The stability constants are evaluated by potentiometry using Ag(I) as competitive ion. In the case of mercury, calorimetric titrations evidence that stability constants are extremely high, and for this reason, they have been determined by means of polarography. Titration calorimetry has been used to determine the reaction enthalpy ($\Delta H°$) and to calculate the entropic term ($T\Delta S°$) allowing the definition of the picture of the complexation

thermodynamics. The results show a higher selectivity for Hg, with respect to other metals, of all the ligands studied in A, whereas this selectivity is lowered in DMSO.

Experimental and theoretical gas phase studies are often useful to interpret at molecular level the thermodynamics of complex formation. In this framework, solution results are compared with gas-phase DFT study on the interaction of 9AneS3 (see pag. 38, Figure 1). Metal solvation has been studied by considering the dissociation of acetonitrile molecules upon ligand coordination. We also checked the effect of introducing continuum solvent model to include the polarization due to the bulk solvent. Results indicate how the observed ligand affinity is a balance of binding and solvent dissociation process.

*Application in process for the extraction of Hg with 9AneS*

The complex formation between the thioether derivative macrocycle 9AneS3 and Hg(II) has been studied by Liquid-liquid distribution technique.

The experiments have been carried out by contacting hexane solutions of 9AneS3 and aqueous $Hg(NO_3)_2$. The results showed the distribution of 9aneS3 between the organic and aqueous phase. Therefore, aqueous insoluble 9AneS3 becomes soluble in presence of aqueous Hg(II) because of corresponding aqueous soluble Hg(II)-9AneS3 complex formation. The analysis of data with LETAGROP-DISTR program has shown the formation of 1:2 and in less extent 1:3 Hg(II):9AneS3 aqueous complexes.

On the other hand, a pre-concentration system including a 9AneS3 impregnated cellulose and polyurethane sponge uses field portable XRF technique which allows the determination of mercury concentration. The results show that the treated cellulose sponge can provide more than one order of magnitude (40 to 50 fold) on Hg concentration with respect to the untreated sponge.

**Ln(III) complex formation with an heterocyclic N-donor ligand**

One of the approaches to obtaining highly emissive complexes is to employ flexible macrocyclic ligands capable of forming a suitable cavity for lanthanide ions and effectively eliminating solvent molecules from the first coordination sphere. This is important in the field of luminescence, which is extensively studied for the lanthanides. For this reason, formation constants for a series of lanthanide and the flexible BTPA (N-donor) (see pag. 86, Figure 26) as complexing agent were determined in AN.

# Riassunto

Il riconoscimento di ioni metallici e lantanidi è di fondamentale importanza in molti settori della chimica e della biochimica, tuttavia i fattori alla base della stabilità e selettività di un legante o recettore specifico sono spesso di non semplice interpretazione. Il processo di riconoscimento può dipendere da vari fattori quali la natura degli atomi donatori e la loro disposizione spaziale, la struttura principale e la rigidità del legante e l'eventuale formazione di chelati con anelli di diverse dimensioni.

**Termodinamica ed estrazione di complessi di metalli pesanti con tioeteri**

Il legame metal - zolfo è una interazione fondamentale nei sistemi biochimici e di separazione selettiva nelle applicazioni per l'estrazione di metalli pesanti e metalli preziosi dalla fase liquida. Ad esempio, numerose strutture macrocicliche contenenti atomi donatori di zolfo (tioli, tioeteri, tiouree, ecc) sono stati usati come estraenti selettivi in una ampia gamma di estrazione con solvente e studi di trasporto attraverso di membrane.

Questa sezione presenta uno studio innovativo sulla termodinamica di formazione del complesso per diverse tioeteri lineari e macrociclico con Zn(II), Cd(II), Hg(II) in solventi organici quali acetonitrile (AN) e dimetilsolfossido (DMSO). Il nostro obiettivo principale è quello di testare il loro potenziale come efficaci agenti complessanti e estraenti selettivi di ioni metallici di rilevanza ambientale e ottimizzare il processo di riconoscimento in un mezzo che ha una costante dielettrica relativamente bassa e che è meno strutturato rispetto all'acqua.

*Termodinamica in soluzione*

I valori delle costanti di stabilità sono ottenuti per potenziometria utilizzando Ag(I) come ione competitivo. Nel caso di mercurio, le titolazioni calorimetrica mostrano che le costanti di stabilità sono molto elevate, e quindi, sono stati determinati con la polarografia. La titolazione calorimetrica è stata usata per determinare l'entalpia di reazione ($\Delta H°$), che

permette di calcolare il termine entropico ($T\Delta S^o$), termini che definiscono la termodinamica della formazione di complessi. I risultati mostrano una maggiore selettività per il Hg, rispetto ad altri metalli, di tutti i leganti studiati in AN, mentre che tale selettività si abbassa in DMSO.

Gli studi teorici in fase gas sono spesso utili per interpretare a livello molecolare la termodinamica di formazione di complessi. In questo contesto, i risultati in soluzione sono confrontati con l'studio in fase gas (DFT) dell'interazione di 9AneS3 (si veda p. 38, Figura 1). La solvatazione del metallo è stata studiata considerando la dissociazione delle molecole di acetonitrile inseguito al coordinamento del ligante. Inoltre è stato introdotto il modello solvente continuo per includere la polarizzazione dovuta alla massa del solvente. I risultati indicano come l'affinità del legante osservata sia il risultato di un equilibrio tra il processo di formazione del legame di coordinazione e quello di dissociazione del solvente.

*Applicazione del processi di estrazione del mercurio con 9AneS3*

La formazione di complessi tra il macrociclo tioetere (9AneS3) e il Hg(II) è stato studiato utilizzando la distribuzione del liquido-liquido.

Gli esperimenti sono stati condotti contattando una soluzione di esano contenente 9AneS3 e una soluzione acquosa contenente $Hg(NO_3)_2$. I risultati hanno mostrato la distribuzione del 9AneS3 tra le fasi acquosa e organica. Pertanto, una soluzione di 9AneS3 insolubile diventa solubile in presenza di una soluzione acquosa di Hg(II), in quanto corrisponde alla formazione di complessi Hg(II)-9AneS3, solubile in acqua. L'analisi dei dati con il programma LETAGROP-DISTR hanno dimostrato la formazione di complessi acquosi 1:2 e in minor misura, 1:3 di Hg(II):9AneS3.

Inoltre, è stato sviluppato un sistema di pre-concentrazione di metalli utilizzando una spugna di cellulosa o poliuretano impregnata con 9AneS3 e successivamente è stata utilizzata la tecnica di "field portable XRF" (FP-XRF), la quale permette la determinazione della concentrazione di mercurio. I risultati mostrano che la spugna cellulosa trattata può

aumentare di più di un ordine di grandezza (da 40 a 50 volte) la concentrazione Hg rispetto alla spugna non trattata.

**Formazione di complessi di Ln (III) con un legante eterociclo N-donatore**

Un approccio per ottenere complessi che emittono altamente nel UV-visble è impiegare leganti macrociclici flessibili in grado di formare una cavità adatta ed efficace per ioni lantanidi eliminando molecole di solvente dalla prima sfera di coordinazione. Questo è importante nel campo della luminescenza, che è ampiamente applicato nello studio dei lantanidi. A questo scopo è quindi di interesse studiare la stabilità in AN di una serie di lantanidi con un legante donatore all'ozoto, (si veda p. 86, Figura 26) come agente complessante.

# Resumen

El reconocimiento de iones metálicos y de lantánidos es de fundamental importancia en muchas áreas de química y bioquímica, pero los factores en base a la estabilidad y la selectividad de un determinado ligando a menudo son de difícil interpretación. Los proceso de reconocimiento puede depender de una serie de factores que incluyen la naturaleza de los átomos donadores y su disposición espacial, la estructura principal y rigidez del ligando y la eventual formación de quelatos con anillos de tamaño variable.

**Termodinámica y extracción de complejos de metales pesados con tioéteres**

El enlace metal - azufre es una interacción fundamental en los sistemas bioquímicos y en aplicaciones de separación selectiva para la extracción de metales pesados y metales preciosos de la fase líquida. Por ejemplo, numerosas estructuras macrocíclicas que contienen átomos donadores de azufre (tioles, tioéteres, tioureas, etc) han sido empleados como extractantes selectivos en una amplia gama de extracción por solventes y estudios de transporte a través de membranas.

En esta sección, se presenta un estudio innovador sobre la termodinámica de la formación de complejos por varios tioéteres lineales y macrocíclicos con Zn(II), Cd(II) y Hg(II) en disolventes orgánicos, tales como acetonitrilo (AN) y dimetil sulfóxido (DMSO). Nuestro principal objetivo es poner a prueba su potencial como agentes complejantes y eficientes extractantes selectivos de iones metálicos de importancia ambiental y optimizar el proceso de reconocimiento en un medio que tiene una constante dieléctrica relativamente baja y menos estructurado que el agua.

*Termodinámica en solución*

Los valores de las constantes de estabilidad son obtenidos mediante potenciometría utilizando Ag(I) como ion competitivo. En el caso del mercurio, las valoraciones calorimétricas muestran que las constantes de estabilidad son muy altas, y por esta razón, se

han determinado con la polarografía. La valoración calorimétrica ha sido utilizado para determinar la entalpía de reacción ($\Delta H°$), la cual permite calcular el término entrópico ($T\Delta S^o$), términos que definen de la termodinámica de formación de complejos. Los resultados muestran una mayor selectividad para el Hg, respecto a otros metales, de todos los ligandos estudiados en la AN, mientras que esta selectividad se reduce en DMSO.

Los estudios teóricos en fase gas son a menudo útiles para interpretar a nivel molecular la termodinámica de la formación de complejos. En este marco, los resultados en solución se comparan con el estudio en fase gaseosa (DFT) de la interacción de 9AneS3 (ver pág. 38, Figura 1). La solvatación del metal ha sido estudiado teniendo en cuenta la disociación de las moléculas de acetonitrilo y la coordinación del ligando. También ha sido introducido el modelo disolvente continuo para incluir la polarización debido a la masa del disolvente. Los resultados indican cómo la afinidad del ligando observada sea el resultado entre el proceso de formación del enlace de coordinación y el proceso de disociación del solvente.

*Aplicación de procesos para la extracción de mercurio con 9AneS3*

La formación de complejos entre el tioéter macrocíclico (9AneS3) y el Hg(II) ha sido estudiada mediante la técnica de distribución líquido-líquido.

Los experimentos se han llevado a cabo poniendo en contacto una soluciones de hexano conteniendo 9AneS3 y una solución acuosa conteniendo $Hg(NO_3)_2$. Los resultados mostraron la distribución de 9AneS3 entre las fases acuosa y orgánica. Por lo tanto, una solución insoluble de 9AneS3 se vuelve soluble en presencia de una solución acuosa de Hg(II) correspondiendo a la formación de complejos Hg(II)-9AneS3, solubles en agua. El análisis de los datos con el programa LETAGROP-DISTR han demostrado la formación de complejos acuosos 1:2 y en menor medida, 1:3 de Hg (II):9AneS3.

Por otro lado, ha sido desarrollado un sistema de pre-concentración de metales utilizando una esponja de celulosa o poliuretano impregnada con 9AneS3 y sucesivamente ha sido utilizada la técnica de “field portable XRF” (FP-XRF), la cual permite la determinación de

la concentración de mercurio. Los resultados muestran que la esponja de celulosa tratada puede aumentar en más de un orden de magnitud (de 40 a 50 veces) la concentración de Hg en relación con la esponja no tratada.

**Formación de complejos de Ln (III) con un ligando heterocíclico N-donador**

Uno de los enfoques para la obtención de complejos que emiten altamente en el UV-visible es emplear ligandos macrocíclicos flexibles capaces de formar una cavidad adecuada y eficaz para los iones lantánidos eliminando las moléculas del disolvente de la primera esfera de coordinación. Esto es importante en el campo de la luminiscencia, que está ampliamente estudiada para los lantánidos. Por esta razón, se determinaron en AN las constantes de formación para una serie de los lantánidos y la BTPA (N-donador) (ver pag. 86, Figura 26) como agente complejante.

# 1. Introduction

## 1.1. Metal toxicity

The toxicity of heavy metals released by a series of productive activities is widely recognized, and therefore the removal from wastewater or the recovery of materials/contaminated water are issues of great importance. The study of the formation of heavy metal complexes for the recognition and separation is a topical issue which is reflected in numerous publications in international journals on fundamental and applied aspects.

Cadmium, copper, lead, mercury, nickel are considered the most hazardous heavy metals and have been used for centuries in a great number of industrial applications. Sources of these metals include mining, agriculture, fossil fuels, metallurgical, chemical and electronic industries, the manufacture and disposal of batteries, paints/pigments, polymers and printing materials [1]. Their release into the environment is a problem of great importance for their adverse effects on the living systems, thus the limitation emission in the environment and the recovery of contaminated areas are particularly important issues today [2, 3].

Hg [4-6] and Cd [7-9] show a strong affinity for ligands such as phosphates, cysteinyl and histidyl side chains of proteins, purines, pteridines, and porphyrins. Hence, these elements can interact with a large number of biochemical sites: all inhibit a large number of enzymes having functional sulfhydryl groups and affect the conformation of nucleic acids. Furthermore these metals are able to disrupt the pathways of oxidative phosphorylation, although in each instance the precise response depends upon the individual properties of the metal.

Hg(II) and organic mercurials interact with -SH and S-S groups of proteins in a multitude of systems, and the consequences for structure and function of proteins have been reviewed

thoroughly. Therefore, the biochemical basis of toxicological effects of Hg and its derivatives are generally sought through mercury-sulfur interactions [4, 5].

On the other hand, the stability constants of the Zn complexes are greater than those of Cd when nitrogen and oxygen-containing groups serve as ligands, but Cd binds more firmly to free sulfur groups. Thus Cd(II) and Zn(II) ions can compete for uptake into various cells and binding to intracellular sites and Cd can displace Zn in a number of biological processes [9]. For example, zinc and cadmium metabolism are related to competitive binding to metallothionein, a low-molecular-weight protein that is involved in the transport and storage of these essential metals (Zn, Cu) [10].

However, from another point of view, the metal ion binding in response to the excessive uptake of metal ions (such as Pb, Cd, and Hg) is a way used by living organisms to protect themselves. For example, the sequestration of these ions by both phytochelatins in plants [11] (they are able to synthesize enzymatically these peptides, which have a high cysteine content) and metallothioneins can play a role in the detoxification of these non-essential metals, prevalently through the coordination of the sulfur atom in the cysteine side-chain [12].

Also Ag(I) has come to prominence for environmental concerns. It is being widely used in metallurgy (alloys) and medicine [13, 14]. Silver nanoparticles are widely used in antibacterial/antifungal agents in biotechnology and bioengineering, textile engineering, water treatment and catalysis [15, 16]. This widespread use of Silver has recently produced some concern about its dispersion in the environment. In fact, recent studies about interactions of silver with essential nutrients, such as Se, Cu, vitamin E and B12, has focused attention also on its potential toxicity [17, 18].

Therefore, the adverse effects of these metal ions for the living organisms have been the motivation for a wide number of experimental [19] and theoretical studies [20-22].

In the last decades, also the increased public exposure to the family of lanthanide metals opens as well the problem of their removal. The biologic importance of the lanthanide ions is because of their similarity to $Ca^{2+}$ ions. All lanthanides show a marked bioinorganic similarity to $Ca^{2+}$ ion, with near equivalence of ionic radii, but with a higher charge density [23, 24]. The lanthanides, display Lewis acid properties which make them useful in the hydrolytic cleavage of phosphor-diester bonds of DNA which, otherwise, is extremely resistant to hydrolysis; cleavage of DNA is an essential step in developing gene therapy [25].

Lanthanides are also used in many applications as electroluminescent devices [26], in lasers [26], catalysis [27] and medicine [23] and their solution chemistry is relevant for the nuclear waste reprocessing since they are an important fraction of nuclear waste which should be separated from actinides in the treatment. The $Ln^{3+}$ ions show very similar chemical properties to the actinides (III) ($An^{3+}$). For this reason, in the design of nitrogen polydentate ligands, L, for application in the field of liquid–liquid extraction and separation of trivalent actinides An(III) from trivalent lanthanides Ln(III) for nuclear waste management, one important goal is to study the mechanism of complexation leading to LnL and AnL complex formation and the thermodynamic properties of these complexes in solution [25].

## 1.2. Methods of extraction from aqueous solutions

For decades the chemical research studied systems for the recognition of heavy metals in order to develop methodologies for selective identification and separation. For example, the design of high-performance adsorbents for environmental clean-up of Hg(II) is highly required, since the acute toxicity for inorganic mercury is very low (from 5 in crustaceous to 800 μg/L in fish) [28], its bioaccumulation in living organisms is high and that its elimination from organisms is difficult.

The basis of these processes is to mobilize the metal in an aqueous phase and concentrate it in a readily treatable phase for the recovery. These two-phase systems are of diverse nature:

the most common involves the transport of metal through a liquid phase (organic) immiscible with water, or through a solid phase [29]. The liquid-liquid technique (LL) [30] involves an immiscible mixture of water and an organic solvent where the metal ion is dissolved in the aqueous layer and the extractant in the organic layer. Another technique refers to the use of liquid membranes that consists on an organic immiscible solvent (the liquid membrane) separating two aqueous phases (the source and receiving phases). For example, the bulk liquid membranes [31], where the organic phase is in direct contact with two aqueous phases in the same container; and emulsion liquid membrane (ELM) [32] where a water-in-oil-in-water system is produced by the use of appropriate emulsifier produces very thin globular membranes of a large surface area per unit source phase volume, which enhances the transport rate of this membrane. Liquid membranes can be found in the micro-porous of polymeric membranes (SLM) [33, 34], where a porous polymeric membrane, impregnated with the organic liquid and carrier, is set in between the corresponding source and receiving aqueous phases. When the polymeric membrane takes the format of a hollow fiber then, the system enhances the surface contact and provides a faster way to separate and concentrate the target elements (HFSLM) [35, 36].

In addition, to obtain favorable results in the mentioned solvent extraction processes it is essential to identifying a compound that has the ability to coordinate one metal selectively and to facilitate transport though the extractant phase. The thermodynamic stability of the metal ion complexes in a given medium is a measure of this selectivity, depending mainly on the geometry and flexibility of the ligand and nature of the donor groups. Therefore, the affinity of a ligand towards a particular metal ion can be determined experimentally from thermodynamic formation constants of the related ligand-metal complex.

In general, such features (acid base properties, structural, constraints, complementarity between the metal ion and the ring cavity) should be evaluated to predict preferential recognition. As mentioned, the affinity of a ligand for a metal ion is determined by the thermodynamic stability constants of formation of ligand-metal complex. The formation constants of a ligand selective for a specific metal use to be orders of magnitude higher than

those competitors. In this way, although the presence of concentrations of competitors can be much higher, a selective ligand will bind and transport only the target ion.

The choice of a ligand selective for a given ion is based essentially on Pearson's hard soft acid base theory (HSAB) [37]. Hard acids and hard bases tend to have the following characteristics: small atomic/ionic radius; high oxidation state; low polarizability; high electronegativity. Soft acids and soft bases tend to have: large atomic/ionic radius; low oxidation state; high polarizability; low electronegativity. Subsequently, the theory has been presented by Pearson and Parr in a more quantitative way (based on Density Functional Theory) [38]. DFT provides an excellent framework, yielding structural information and a number of chemical reactivity indices about ligands and their metal complexes, and gives results of quality comparable to those obtainable by correlated *ab initio* calculations [39].

On the basis of this theory, ions classified as hard (e.g. lanthanides(III), actinides, Al(III), Fe(III), alkali metal ions) give strong complexes with hard ligands like O-donors (carboxylates, carbonyls..) and N-donors (amines). Soft metals (Hg(II), Pt(II), Pb(II), Ag(I), …) form strong complexes with soft ligands like S donors (e.g. tiols, tioethers). Therefore, the design of a selective chelating ligand based on this classification is of capital importance. Structural features of the chelator also contribute to the stability of the complex and the selectivity for a given metal: the chelation type (size of the ring), the match between the size of the metal ion and the cavity (for macrocyclic ligands), the steric impediments of the complex formed.

## 1.3. Scope of the thesis

From the introduction section it clearly emerges that thermodynamics of metal-ligand formation is a key factor for the interaction with both biological and synthetic ligands. This fact reveals the detailed description of the metal ligand interaction to be fundamental both to understand the biological effects of these metal ions and to develop efficient methods for metal separation.

Taking into account the background described, the **first objective** of the present thesis is to carry out a thermodynamic study of the interaction of a series of sulfur-containing ligands (linear and cyclic thioethers) (see Figure 1) with heavy metals (Ag, Cd, Hg) which can be interesting both for a deeper understanding of the interactions with bio-ligands and for the development of extraction processes from solutions. This will proceed through the assessment of the thermodynamic parameters of formation of the complexes between a series of thioethers and the heavy metals in organic solvents using experimental techniques such as thermodynamic, electrochemical and theoretical methods.

In this context, some data exist on structures or NMR characterization of heavy metal compounds with sulfur containing ligands [40, 41], less numerous are those regarding their stability. The work has been extended also to the study of complexation of the essential $Zn^{2+}$ ion, in order to compare the coordination properties of soft and hard $d^{10}$ metal ions toward the sulphur donors.

Taking advantage of the obtained knowledge, tests of the two-phase separation systems have been carried out using various configurations already described (ligand, phase extractant and support).

**Specific objectives:**

- ✓ Thermodynamic characterization of chemical affinity of a series of linear and cyclic thioethers in non aqueous solvents (acetonitrile and dimethyl sulfoxide) using calorimetric and potentiometric techniques and correlation with the structure and solvation of the heavy metals.

- ✓ Determination of thermodynamic parameters and redox properties of mercury complexes using electrochemical techniques.

- ✓ Determination of metal complexes formation by using two phase equilibrium systems.

- ✓ Development of analytical applications of the studied metal complexes by using appropriate supports to facilitate selective metal adsorption, i.e., cellulose and polyurethane impregnated sponges for selective separation and pre-concentration of mercury.

The **second objective** of this thesis, is the study of the complex formation of lanthanides with N-donor chelants (TPA and BTPA) (see pag. 86, Figure 26) and the determination of the stability constant values and their variation along the series. This is motivated by the fact that heteroaromatic N-donor ligands have been previously proposed as extractants (see pag. 86, Figure 26, BTP derivatives, terpy) in nuclear waste reprocessing and also for the potentially interesting luminescence properties of $Ln^{3+}$ complexes with this ligand in solution. Despite these potential interesting applications there is a limited number of thermodynamic studies of complex formation of lanthanides with heteroaromatic N-donor ligands.

# 2. Thermodynamics and extraction of heavy metal complexes with thioethers

## 2.1. Solution thermodynamics

### *2.1.1. Introduction*

Cations can exert strong attractive action towards negatively charged or polar groups of ligands. This leads to the formation of a covalent bond between the ligand and the metal ion.

In the coordinate covalent bond formed in the complex, the metal ion is the acceptor of electron pairs, while the ligand acts donating electron pairs to establish the bond.

$$mM^{a+}\text{ (acceptor)} + nL^{b-}\text{ (donor)} \leftrightarrows [M_mL_n]^{(a-b)}\text{ (complex)} \tag{2.1}$$

In eq. (2.1) if b = 0 the ligand is neutral. If in eq. (2.1) m = 1 the complex is called mononuclear. Therefore, the formation of complex can be explained by the acid-base theory of Lewis. Thus, the central ion is an acceptor of electron pair or Lewis acid and each ligand a donor of electrons pairs or Lewis base.

The stability of a complex is quantitatively defined from the formation constant (*K*) for reaction (2.1). This constant is expressed by the equation (2.2) (charges omitted):

$$K = \frac{[M_mL_n]}{[M]^m[L]^n} \tag{2.2}$$

More complete information for the thermodynamic characterization of a complex can be obtained from the thermodynamic parameters associated with the formation constant, that

is, the change of standard Gibbs free energy (ΔG°), enthalpy (ΔH°) and entropy (ΔS°) for the reaction considered.
The formation constant for any reaction is related to the corresponding free-erengy changer by the expression (2.3):

$$\Delta G^o = - RT \ln K = \Delta H^o - T\Delta S^o \qquad (2.3)$$

Where R is the gas constant ($R = 8.31\ J \cdot mol^{-1} \cdot K^{-1}$) and T is temperature in Kelvin.

The corresponding change of entropy (ΔS°) is obtained (eq. 2.3) by the ΔG° and the enthalpy change of complex formation, which is best measured calorimetrically. Analysis of *K* into their component heat and entropy terms is essential to the ful understanding of the many factors (such as the size, shape, and electronic structure of central group and the ligand, the temperature, and the composition of the solvent) which influence the stability of a complex [42, 43].

### *2.1.1.1. Effect of the solvent*

An important property of a solvent is its dielectric constant that can be considered as a measure of neutralization when ions interact with a solute or opposed ionic substances. The smaller the dielectric constant, the greater the attractive forces between the opposite solute ions, and consequently, in solvents with low dielectric constant (less than 15) the interactions between ions have a wider space and they are mostly associated. The concentration of ions in solution is negligible compared to the other molecules in solution. In solvents of high dielectric constant (ε), ionic bonds are broken completely and the ion pairs are fully dissociated. This happens in water ($\varepsilon = 78.36$) and, in general, in solvents with $\varepsilon > 40$ [44] .

The reaction medium is an important factor determining the nature and stability of the species formed due to the contribution of the solvation/desolvation processes to the

thermodynamic parameters. In solution, we can consider this as a competitive reaction between solvation desolvation of the metal ion and of the ligand and the formation of the complex. In fact, under the hypothesis of complete dissociation of the metal salt in a given solvent, the reaction (2.1) involves the solvated metal cation as reagent and can be rewritten:

$$m[MS_i]^{a+} + nL^{b-} \leftrightarrows [M(S_j)L_n]^{(a-b)} + (i-j)\ S \qquad (2.4)$$

(S = solvent molecule)

It is straightforward to understand that the strength of the metal-solvent bond is accounted in the energetic balance which determines the values of the thermodynamic parameters of reaction. A factor which does not emerges from reaction (2.4), but is present in the experimental situation, is that also the ligand interacts with solvent with relatively weak interactions (coulombic, dipolar, van der Waals, H-bonding). In vacuum, this competitive process is absent and an absolute affinity of a ligand for a metal ion can be measured (or calculated). For example the so-called "anomalous order" of the basicity scale of amines in water (i.e., $NH_3$ < primary < secondary > tertiary), is in contrast with the order found experimentally in gas phase and expected for the inductive contributions of the substituents (tertiary > secondary > primary > $NH_3$). This effect, also observed for the formation of complexes with several ions (e.g. $Ag^+$), is explained of the basis of the interaction of amines with water molecules through hydrogen bonding [45].

Reaction (2.4) is helpful for interpreting the fact that metal complexes with the same ligand in different solvents can have log*K* values differing of several orders of magnitude and markedly different enthalpy values (even of opposite sign). When comparing two metal ions also selectivity of the same ligand can change in different media.

At the moment, most of the literature on thermodynamics of metal complexes in solution to characterize the carrier has been focused on aqueous solutions, while little has been studied in organic solvents, although representing a more similar environment (low dielectric

constant, absence of protonation equilibrium, possible ionic associations) in which the metal exists in the organic phase of extraction processes. For this reason, this first chapter presents the study focused on determining the thermodynamic properties of the complexes formed between heavy metals and S-donor ligands using acetonitrile (AN), a low dielectric constant medium ($\varepsilon = 35.94$) [44]. In addition, the study has also been extended to the more coordinating solvent dimethyl sulfoxide (DMSO, $\varepsilon = 46.45$) [44].

### *2.1.1.2. Crown thioethers*

As previously discussed in the general introduction, sulfur is an ubiquitous element of particular environmental and biochemical importance with many vital functions in proteins and enzymes.

The employment of polythioethers for the complexation of Hg(II) and other toxic or precious soft metal ions is based upon their known high affinity for mercury since they are soft ligand donors according to the HSAB theory [37, 46]. Thiacrown ligands (and their derivatives) could be utilized as selective complexing agents for the removal and transport of heavy metal ions as demonstrated in by Baumann and coworkers [47] who prepared a pentathiacrown that was attached to a polystyrene polymer able to remove Hg(II) up to 99% or higher. In addition to the removal of Hg(II) in wastewater remediation applications, another important and relevant use of mercury coordination chemistry with macrocyclic ligands is the detection and quantitative measurement of the heavy metal ion itself, for example by fluorescence measurements [48].

Although acyclic thioethers are not very good binders, crown thioethers are important ligands, especially for late transition metals. The properties of crown thioethers have been attributed to assumed conformational preferences, largely based on X-ray studies of the ligands and their complexes in the solid state [2, 46, 49].

The functional ability of the crown compounds is generally based on the cavity size of a ring, the molecular structure, the number and the nature of donor atoms (in case that the

thioether group is not the only one present in the ligand scaffold). With increasing dimension of the crown ether the flexibility can be an important factor in determining the selectivity for a given metal ion. For example, it has been pointed out [46] that in the solid state thiacrown ethers have the ability to force rare geometries on the heavy metal ion ($Hg^{2+}$) [46]. For example, square planar (S4), square pyramidal (S5), and octahedral (S6) geometries have been reported, that contrast the more common four-coordinate tetrahedral and two-coordinate linear geometries typically seen for Hg(II) complexes [46].

Ligands containing thioether groups show a considerable increase in complexation stability with soft metal ions such as $Ag^{+}$ and $Hg^{2+}$ ions in solution [50-52], but there is a lack of systematic quantitative thermodynamic data on this type of complexes. Especially interesting comparisons should be possible between the monovalent $d^{10}$ acceptor Ag(I), with very soft character, and the divalent very soft Hg(II) or borderline Cd(II).

In this thesis, three cyclic thioethers and one linear thioether have been considered (see Figure 1): 1,4,7-trithiacyclononane (9AneS3); 1,4,7,10-tetrathiacyclododecane (12AneS4); 1,4,8,11-tetrathiacyclotetradecane (14AneS4); dietyl sulfide ($Et_2S$). These macrocyclic ligands are free of any protonation consideration and hardly soluble in water.

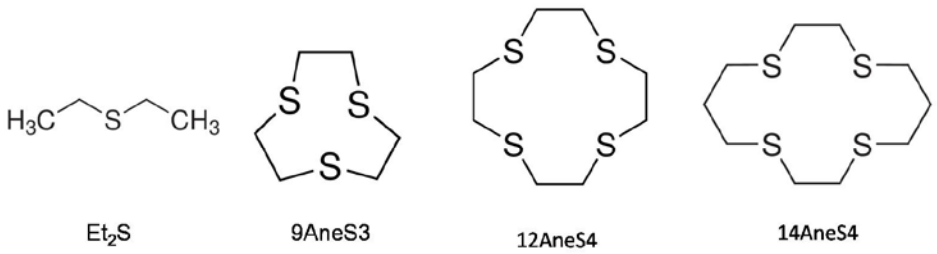


Figure 1 Linear and macrocyclic thioethers

### *2.1.2. Experimental*

#### *2.1.2.1. Chemicals*

Zn(II) and Cd(II) anhydrous perchlorates to be used in AN were prepared according to the described procedures [53]. Also $Zn(ClO_4)_2 \cdot 6DMSO$ and $Cd(ClO_4)_2 \cdot 6DMSO$ were prepared as previously described [53]. Anhydrous mercury perchlorate was obtained from $HgClO_4 \cdot 3H_2O$ (Aldrich) by drying at 30°C for 1 week under vacuum in presence of $P_2O_5$. Anhydrous silver perchlorate was obtained from $AgClO_4 \cdot H_2O$ (Aldrich) as described [53]. The thioether ligands (Aldrich) were previously dried. The solvents, AN (Sigma-Aldrich >99%) and DMSO (Aldrich 99%) [54] were purified by distillation. Successively, solvents were transferred in a glove box and stored in presence of molecular sieves.

Perchlorate stock solutions of Zn(II), Cd(II), Hg(II) (and Ag(I)) ions and thioethers ligands were prepared by dissolving in anhydrous degassed DMSO or AN weighed amounts of the adducts (or of the anhydrous $AgClO_4$) and their concentrations were checked by titration with EDTA [55], with the exception of mercury, which has been determined by weighing. Concentrations calculated by weight were quite reliable since for Cd and Zn perchlorates the value determined by EDTA titration and weighting were nearly the same. The background salt ($NEt_4ClO_4$) was prepared according to the described procedures [53].

All standard solutions were prepared and stored in a MB Braun 150 glove box under a controlled atmosphere containing less than 1 ppm of water and less than 1 ppm of oxygen. The water content in the solutions, typically 1-10 ppm, was determined by a Metrohm 684 KF Coulometer.

#### *2.1.2.2. Potentiometry*

The potentiometric titration technique was used to determine the stability constant of complex formation with silver (I) (as perchlorate) in AN. The potentiometric titration is a technique, where the voltage change across the analyte, typically an electrolyte solution is

measured. Emf of the cell depends on the concentration of the electrolytes with which the electrodes are in contact. As the concentration of analyte changes, the emf of the cell also changes correspondingly. Thus the potentiometric titration involves the measurement of emf between an indicator electrode and a reference electrode, with the addition of titrant (Figure 2).

The potentiometric titrations were performed with an automatic burette. All titrations were carried out in constant ionic strength, with an electrolyte solution of 0.1 M $Et_4NClO_4$ and working under nitrogen atmosphere at 298.15K. The solution was allowed to reach the equilibrium within 90 seconds after each addition of titrant. The automatic titrator was connected to a computer, which controlled the addition of titrant.

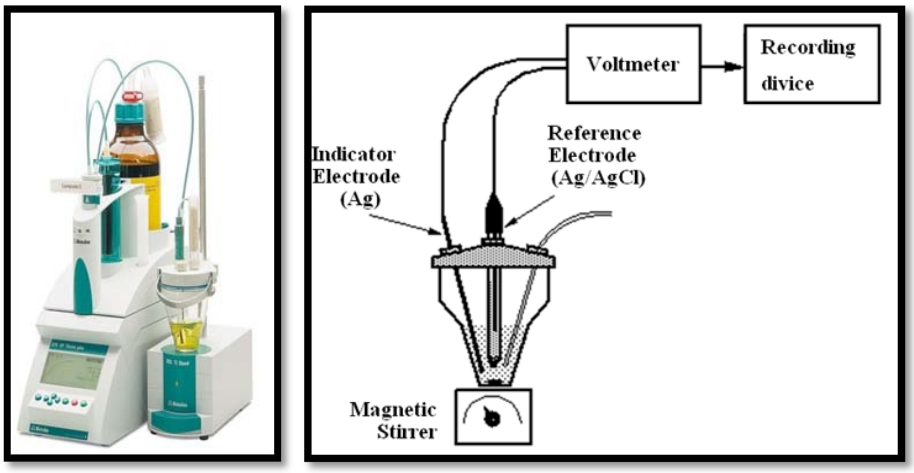


Figure 2 Potentiometric titration instrument (left).Scheme of the reaction cell (right)

The following cell (2.5) has been employed for the determination of the stability constants of $Ag^+$ complexes, equipped with a reference electrode (Ag/AgCl) and a silver indicator electrode.

$$Ag|C_{Ag}, C_L, C_M||AgClO_4(0.1M)|Ag \qquad (2.5)$$

Where, $C_{Ag}$ , $C_L$, $C_M$, are the concentrations of silver, ligand and metal competitor in AN solution in the cell. When the stability constants with $Ag^+$ were determined, the competitor metal ion M was absent.

For the determination of the stability constants with $Zn^{2+}$ and $Cd^{2+}$ the "competitive method" [42] has been employed using $Ag^+$ as competitor. This method requires that the stability constants of a given ligand with the competitor are already known by previous experiments. Then, a solution containing the cation ($Zn^{2+}$, $Cd^{2+}$) and the competitor was titrated with the ligand solution and the emf was recorded. Computer data fitting, using the program Hyperquad [56], allows to determine the stability constants of the studied cations.

In the case of Hg(II), competitive potentiometric titration using Ag(I) could not be carried out, because of a concomitant redox reaction occurring in solution. For this reason, the stability constants were determined by polarography (see section 2.1.2.4). This last methods was chosen as calorimetric and UV-Vis experiments evidenced a very high stability for Hg-thioethers systems in AN.

### *2.1.2.3. Calorimetriy*

A Tronac model 87-558 precision calorimeter (Figure 3) was employed to measure heat exchange for the reaction in order to calculate enthalpy values ($\Delta H^o$) and entropy terms ($\Delta S^o$) from equation (2.3). The calorimeter consists of the following parts: a jacket or bath, which surrounds the calorimeter and whose temperature is kept constant throughout the measurement process; a contact thermometer to adjust the bath temperature; an auxiliary heater that supplies power to the bath, two agitators one for bath and one for cell; a heating pad which supplies power to the cell; a Dewar flask containing the substance in question and a burette containing the titrant.

Figure 3 Tronac model 87-558 precision calorimeter.

In Figure 4 the scheme of the calorimetric cell is shown. The calorimeter is equipped with a 5 mL burette connected by a teflon tube to the reaction vessel. The system was submerged in a thermostatic water bath at 298.15 K and allowed to reach thermal equilibrium. Then the solution of metal in the cell reaction is titrated with the solution of ligand. Great care has been paid to avoid the presence of water in DMSO, and particularly, AN solution.

The usual titration procedure consists in a continuous addition of titrant solution. As the volume delivery rate is known (by previous calibrations) and the time is measured by the control software, the volume added at every time is precisely determined. The temperature of the system (relative to that of the thermostated bath) is recorded at fixed time intervals. As we are interested in the heat produced/absorbed during the reaction we need to know the heat capacity of the system. The "energy equivalent" (i.e. the heat capacity) of the system is determined by a series of calibrations prior to the experiment and at the end of it. During a calibration, a resistance (electric calibration) delivers a

known amount of heat in the vessel for a known amount of time. The temperature change is simultaneously monitored and the energy equivalent can be calculated. Our control software also calculates the heat produced at each titrant volume added (temperature is recorded at fixed time intervals, generally ~5 sec.).

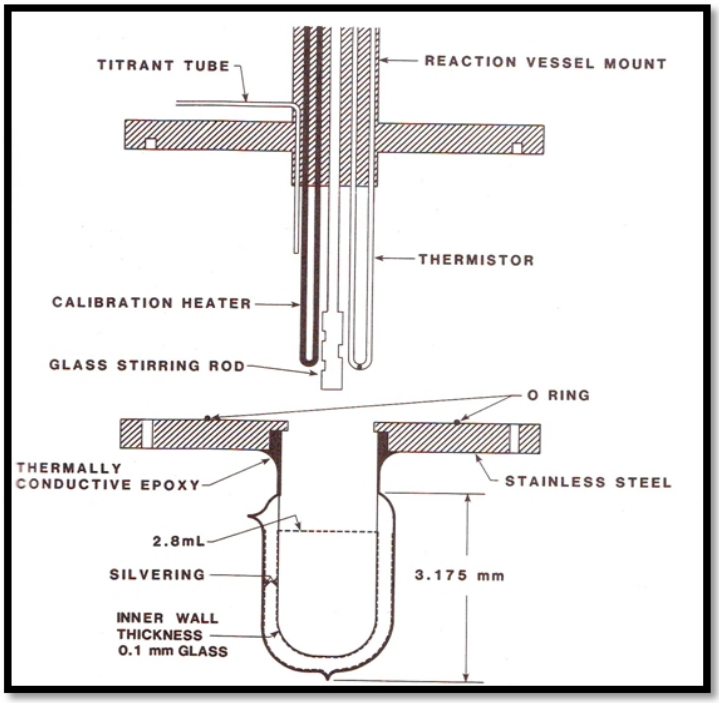


Figure 4 Design of titration isoperibol solution calorimeter reaction vessel.

The reproducibility of the equipment has been tested with the reaction of protonation of an aqueous solution of tris(hydroxymethyl)aminomethane (Tham) with hydrochloric acid (HCl, 0.1 mol·dm$^{-3}$) at 298.15 K. The value determined -47.50 ± 0.08 kJ.mol$^{-1}$ is in accordance with the environment reported by Hill, et al. [57] using a reaction calorimeter LKB.

Heat data obtained allows the determination of the stechiometry, the enthalpy of formation ($\Delta H^o$) and, in some cases, the formation constant (K). Once the raw heat data

were collected, the enthalpy calculations were performed using the program HyperDeltaH [58]. In general, standard enthalpy of complexation were calculated using fixed values of log*K* (previously determined by potentiometry of polarography).

### *2.1.2.4. Polarography*

To verify the formation of complexes between the ligands L and the ion $Hg^{2+}$ polarography has been used, that is an electrochemical technique where a potential linearly variable in time is applied to a dropping mercury electrode while the developing current is measured. This technique allows to obtain same important parameters of the redox processes between the species in solution and the electrode surface as the number of involved electrons, the stoichiometry of the reactions and the approximated value of E°. In fact, if the diffusion coefficients of the reduced and oxidized species are similar, $E° = E_{1/2}$ (see equation (2.6)), where $E_{1/2}$ is the potential value when the current is half of its limiting value.

The working electrode is a dropping mercury electrode that is formed by a head of Hg 20 to 100 cm high connected to a glass capillary with a cross section of a few tenths of mm. The mercury was previously purified by repeated washing with dilute $HNO_3$ and $H_2O$, drying and reduced-pressure tri-distillation.

The calibration was done using salts of $Cd^{2+}$ as standard and the reduction reaction $Cd^{2+} + 2e^- \rightarrow Cd$ (amalgam). The resulting polarographic wave is sigmoidal in shape as predicted by theory for many cations as $Cd^{2+}$ in water and in the presence of strong supporting electrolytes. In the present case the $Cd^{2+}$ salt was added to a solution containing $NaClO_4$ 0.1 M at 25 °C and shows $E_{1/2}$ = -0.63 V vs. SCE: the polarographic analysis of the obtained wave gives exactly $2e^-$ reduction.

The polarographic measurements were performed in a thermostated jacked cell with five necks holding three electrodes: (Figure 5)

1) reference electrode (RE): Ag|$AgNO_3$ (0.01 M in acetonitrile), TEAP (0.1 M); the electrode was separated by the solution by a vycor frit to avoid ion contamination.
2) counter electrode (CE): Pt wire directly dipped in the solution.
3) working electrode (WE): dropping mercury electrode, AMEL 460/30".

A knocker of 1 s assures the reproducibility of drop life time.

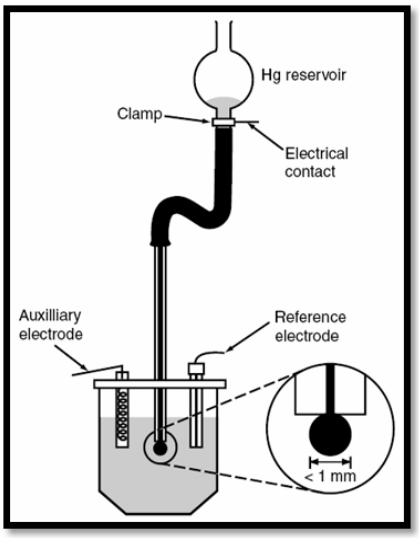


Figure 5 Assembly of the cell

The circuit is controlled by a potentiostat that allows the potential variation between WE and RE, but switches the current between WE and CE. In this way no current flows between WE and RE and so there is no potential drop between them (RI, Ohm's law). The potential of the working electrode is expected not be influenced by the resistance of the solution that is generally high in non aqueous solvents as AN.

$V_{applied}$ = V on the electrode - IR potential drop (due to the resistance of the solvent and the flowing currency that is not constant).

If RI = 0 then $V_{applied}$ = V on the electrode surface.

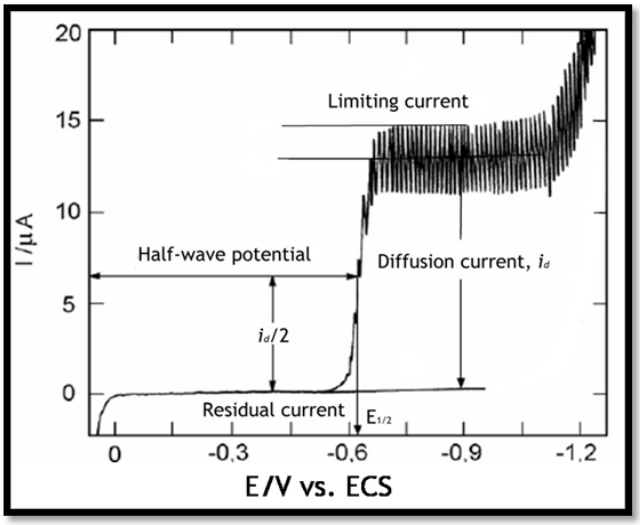


Figure 6 Polarographic wave

The polarography allows the investigation both of reductions and oxidations of electroactive species in solution. The obtained signals have a classical sigmoidal form as it is reported in Figure 6 where a reduction process is considered. At the increasing of WE potential towards more negative values, a cathodic current develops whose height increases with the variation of V up to a maximum limiting value and then becomes constant. The condition of limiting current is due to the fact that the reduction rate is due to two chained phenomena: 1) the electron transfer between electrode surface and species in solution through the electrical interface and 2) the diffusion of the consumed species from the bulk of solution to electrode surface. Generally the diffusion is the rate determining step of the all process. When such condition is reached the current is called limiting diffusion current $i_L$ or $i_d$.

In the case studied in this work, the WE potential is varied from negative to more positive values (anodic sense) in order to see the developing of anodic current signals due to the oxidation of species in solution. In this case, the polarographic wave for the oxidation is expressed by the equation (2.6).

$$E = E^0 + \frac{RT}{2F} ln\left(\frac{id - i}{i}\right)\left(\frac{D_{ox}}{D_{red}}\right)^{1/2} \quad (2.6)$$

The experiment was always done in the following procedure. The solvent was acetonitrile (3 mL) which has been freshly distilled and then stored on molecular sieves. Tetraethylammonium perchlorate ($NEt_4ClO_4$), at a concentration 0.1 M, was added as supporting electrolyte: its presence is necessary to maintain a constant ionic strength and to minimize migration of charge species: in this way diffusion is the only force that the species in solution feel. The potential scans were carried out at a scan rate of 5 mV/s in the operating range, dropping time of 1 s, in nitrogen atmosphere (bubbling $N_2$ for 10 min) and at room temperature, approximately 25 ºC. The background was always recorded and in these conditions the signal of the bielectronic oxidation of the mercury (2.7) with a positive potential is seen.

$$Hg \rightarrow Hg^{2+} + 2e^- \quad (2.7)$$

Also a second oxidation reaction develops and is attributed to equation:

$$2Hg \rightarrow Hg_2^{2+} + 2e^- \quad (2.8)$$

When there is no ligand in solution the ratio of concentrations of $Hg_2^{2+}/Hg^{2+}$ = 120/1. When the ligands were present the species formed are mainly $[HgL_x]^{2+}$ [59]. In a typical experiment a weighed quantity of ligand was added to the solution. In a polarographic measure, we observe the formation of polarographic oxidation wave, which is described by the equation (2.9).

$$Hg + xL \leftrightarrows [HgLx]^{2+} + 2e^- \quad (2.9)$$

Where L is the ligand and x is the stoichiometric coefficient.

The relationship between the half-wave potential of the process and the stability constant (2.10).

$$K = \frac{[HgL_x]^{2+}}{[Hg^{2+}][L]^x} \tag{2.10}$$

is expressed as:

$$E_{1/2} = E^0 - \frac{RT}{2F} lnK + \frac{RT}{2F} ln\left(\frac{2^{(x-1)}\sqrt{D_L}}{x[L]^{(x-1)}\sqrt{D_C}}\right) \tag{2.11}$$

Where E° is the formal potential of the couple $Hg/Hg^{2+}$ vs. the reference electrode (+0.572), $D_L$ and $D_C$ are the diffusion coefficients of the free ligand and the complex, respectively [60-62].

According to the equation (2.11) you can determine the constant of complex formation. However, the following points should be underlined:

- when $E_{1/2}$ depends on the concentration, the stoichiometry of the reaction is 1:2 and the formation constants obtained from the following equation:

$$E_{1/2} = E^0 - \frac{RT}{2F}\left[lnK + ln\left(\frac{[L]}{2}\right)^{(x-1)}\right] \tag{2.12}$$

  where x = 2 and $E^o$ = +0.572

- when $E_{1/2}$ does not depend on the concentration, the stoichiometry of the reaction is 1:1 and the formation constants obtained from the following equation:

$$E_{1/2} = E^0 - \frac{RT}{2F} lnK \tag{2.13}$$

  where x = 1 and E° = +0.572

### *2.1.2.5. Theoretical calculations*

Experimental and theoretical gas phase studies are often useful to interpret at molecular level the thermodynamics of complex formation. The reaction of $M^{2+}$ ions with 9AneS3 and $Et_2S$ has been studied by means of DFT calculations using three different functionals. Geometry optimizations carried out in vacuum using a 6-31+G(d) basis set for all atoms (H, C, N and S) except the metal ion. The metal ions were described by the quasi-relativistic Stuttgart-Dresden pseudopotential and the relative basis set. Stationary points were characterized by vibrational mode analysis. The reliability of the results has been checked by comparing calculated structures to experimental counterparts. All calculations were performed with Gaussian09 program [63].

### *2.1.3. Results and discussion*

The thermodynamic study of the complexes formed between thioether ligands and heavy metals (Ag(I), Zn(II), Cd(II) and Hg(II)) were carried out through the techniques explained in the section 3.1.2.

#### *2.1.3.1. 1,4,7-trithiacyclononane (9AneS3)*

The 9AneS3 (Figure 1) is the smaller cyclic thioether with three S-donor atoms (tridentate). This has been the most widely investigated because of its good solubility in AN along with the fact that (as it will be described later) it is the only able to from stable complexes with all the metals considered in this work.

Figure 7 shows the potentiometric curves in form of potential variation ($\Delta E = (E_{meas} - E_{initial})$) *vs.* the ratio of the concentrations of ligand to metal ($C_L/C_M$).

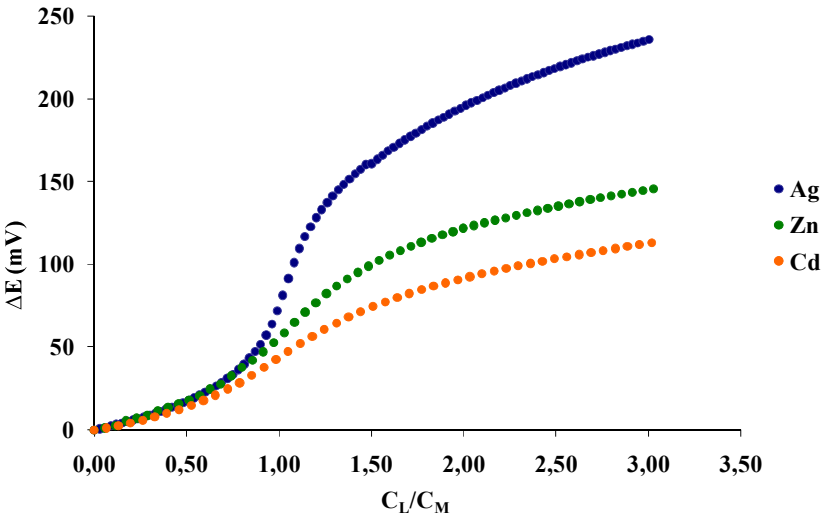


Figure 7 Competitive potentiometric titration for 9AneS3 ($2.63 \cdot 10^{-2}$ M). Concentration of metals are Ag(I) = $1.5 \cdot 10^{-3}$ M (without the presence of competing metal), Ag(I) = $1.5 \cdot 10^{-3}$ M (with the presence of competing metal) and Zn(II) and Cd(II) = $8 \cdot 10^{-3}$ M in AN.

The curves represent the potential, which is related to the concentration of ion sensitive to the electrode through the well known Nernst equation [42]. Therefore, a lower curve indicates a higher concentration of free Ag(I) showing the formation of stable 9AneS3 complexes with the ion in competition. This is observed for the two metals (Zn(II) and Cd(II)) being more evident in the case of Cd(II), with which more competition and therefore more stable complexes are indicated.

As an example, Figure 8 shows the polarograms of background signal corresponding to the bielectronic oxidation of mercury (2.8) in absence of 9AneS3, and the polarographic wave resulting from the reaction (2.9) which the formation of the Hg-9AneS3 complex occurs. In presence of 9AneS3 a change in the $E_{1/2}$ to negative values is appreciated.

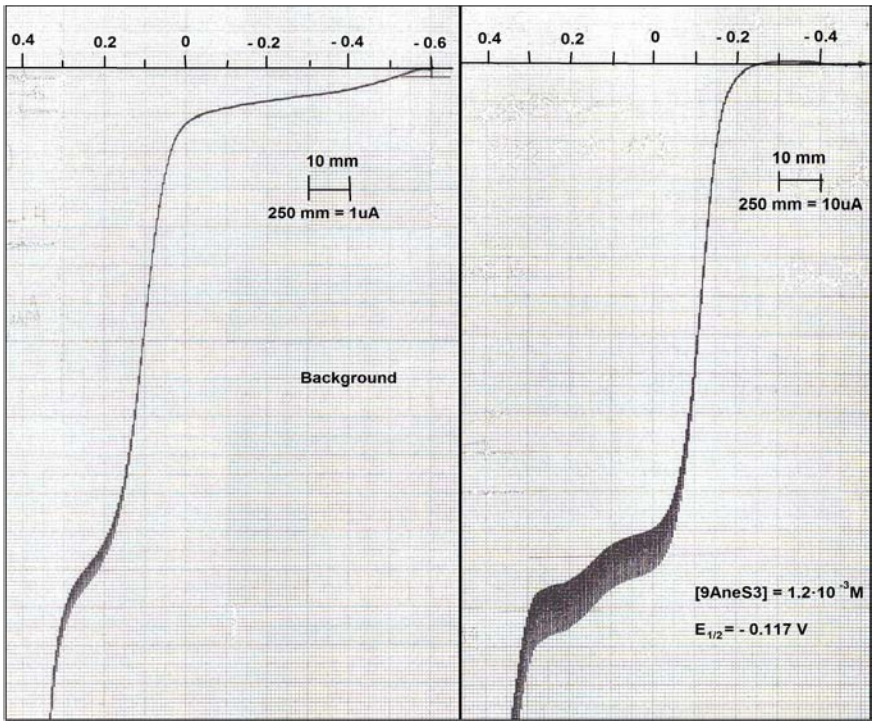


Figure 8 Polarographic waves in absence of ligand (background) (left) and in presence of 9AneS3 ($1.2 \cdot 10^{-3}$ M) (right) in AN.

The experiments with 9AneS3 and Hg(II) show a polarographic wave with $E_{1/2}$ variable in the range of concentrations analyzed ($1.02 \cdot 10^{-2}$ M - $4.8 \cdot 10^{-4}$ M), changing to more positive values with decreasing concentration. Therefore, the least squares fit of the logarithm of the concentration of the ligand (log ([L]/2)) versus the half-wave potential ($E_{1/2}$) (Figure 9) determines the 1:2 complex formation constant with a value of $\log\beta_2 = 25 \pm 1$ (see equation (2.12)).

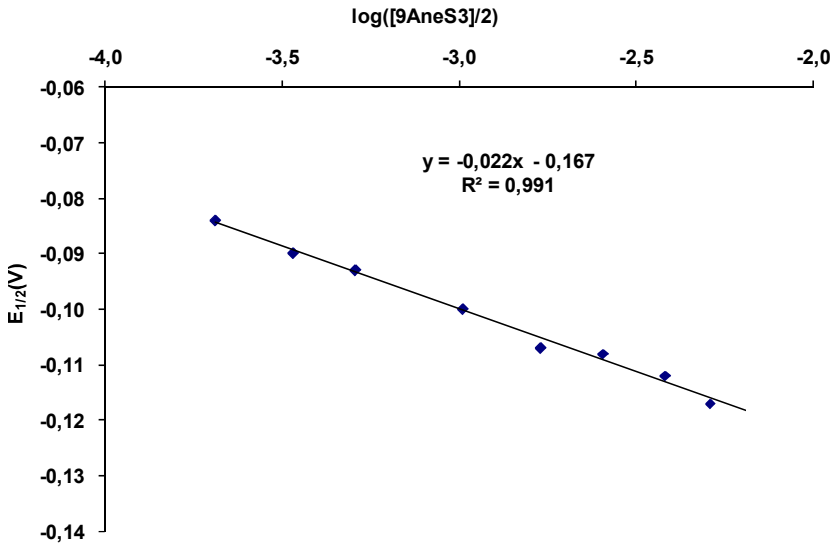


Figure 9 Plot of log ([L]/2) vs. $E_{1/2}$ for 9AneS3 with the best fit interpolation line in AN.

The calorimetric data of each metal with 9AneS3 are reported in
Figure 10. The experimental data show, in all cases, that the 9AneS3 form ML and $ML_2$ complexes. More specifically, and especially for Hg(II), the strong ML complex formation is indicated by the linear increase of the curves to a value of $C_L/C_M$ equal to 1. On the other hand, and only for the case of Hg(II), a change in the slope of the curve to a value of $C_L/C_M$ equal to 2 is observed, indicating also the formation of a strong $ML_2$ species. The behavior of the other metals is rather different, since they form a markedly weaker second complex.

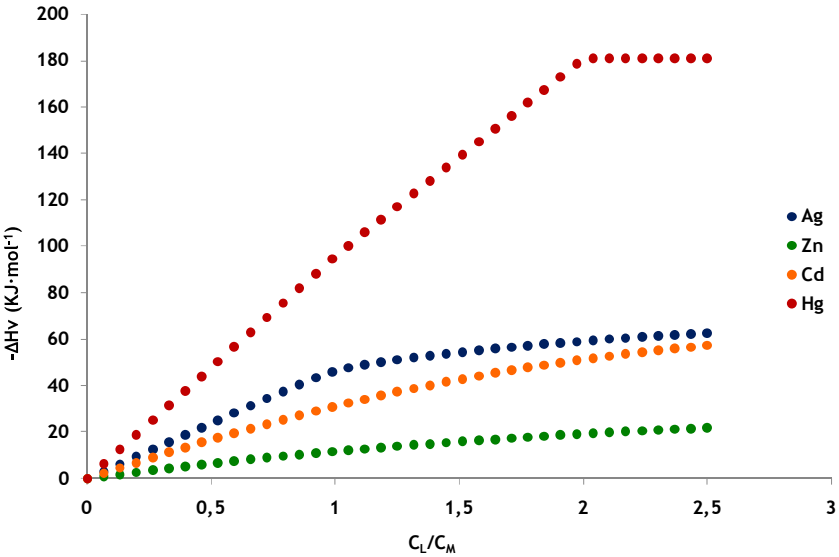


Figure 10 Calorimetric titration for 9AneS3 ($2.63 \cdot 10^{-2}$ M) with all metal ($3 \cdot 10^{-3}$ M) in AN.

The enthalpies of solvation of these metal ions in AN follow the order: Zn(II) < Hg(II) < Cd(II) ($-\Delta H_{sv}$ = 2043, 1851 and 1819 kJ·mol$^{-1}$) [64] being the values for Hg(II) and Cd(II) very close to each other. The calorimetric results do not follow this trend indicating that also a significant different intrinsic affinity of the metal ions for the 9AneS3 ligand must be taken into account. The thermodynamic data are presented in Table 1.

All the complexes are enthalpy stabilized and entropy destabilized, with a selectivity order following the trend Hg >> Ag > Cd ~ Zn.

All entropy terms are negative, as typically found for the formation of complexes with neutral ligands in organic solvents. Also entropy terms are all negative and indicative of a lack of compensation between the loss of degrees of freedom of the ligand and the cation and the entropic gain due to the release of solvent molecules. While for bivalent metals the enthalpic data are quite clear in indicating the relative affinity for the three metals, the entropy results for the 1:1 species are quite puzzling as it becomes more negative from zinc to cadmium, then is more positive for mercury. The last could be due to the imprecision on

the $\log\beta_1$ of Hg(II) complex which has been only estimated on the basis of calorimetric data and of the value of $\log\beta_2$ determined by polarography.

Table 1 The thermodynamic data for 9AneS3 in AN.

| | **log β** | **-ΔG°** **(kJ/mol)** | **-ΔH°** **(kJ/mol)** | **TΔS°** **(kJ/mol)** |
|---|---|---|---|---|
| **$Ag(9AneS3)^+$** | 5.89 (±0.01) | 33.6 (±0.1) | 48 (±1) | -14.4 |
| **$Ag(9AneS3)_2^+$** | 8.88 (±0.01) | 50.7 (±0.1) | 79 (±3) | -28.3 |
| **$Zn(9AneS3)^{2+}$** | 3.10 (±0.01) | 17.7 (±0.1) | 26 (±2) | -8.3 |
| **$Zn(9AneS3)_2^{2+}$** | 5.38 (±0.04) | 30.7 (±0.2) | 49 (±5) | -18.3 |
| **$Cd(9AneS3)^{2+}$** | 3.66 (±0.03) | 20.9 (±0.2) | 44 (±1) | -23.1 |
| **$Cd(9AneS3)_2^{2+}$** | 6.80 (±0.06) | 38.8 (±0.3) | 77 (±2) | -38.2 |
| **$Hg(9AneS3)^{2+}$** | 16* | 92* | 96 (±2) | -4 |
| **$Hg(9AneS3)_2^{2+}$** | 25 (±1) | 143 (±6) | 181 (±3) | -38 |

* Estimated value from calorimetric data.

### *2.1.3.2. Origin of the selectivity of 9AneS3*

Due to the structural simplicity of the ligand and the availability of a complete set of thermodynamic data for the formation of complexes with 9AneS3, a complementary theoretical study of the complexation has been also carried out in order to investigate on the possible reasons of the ligand selectivity.

In Figure 11 are reported the calculated enthalpy changes for coordination of 1 and 2 molecules of 9AneS3 in gas phase (no solvent effect), as described in the reactions (2.14) and (2.15).

$$M_{(g)}^{n+} + 9AneS3_{(g)} \rightarrow M(9AneS3)_{(g)}^{n+} \quad (2.14)$$

$$M(9AneS3)_{(g)}^{n+} + 9AneS3_{(g)} \rightarrow M(9AneS3)_{2(g)}^{n+} \quad (2.15)$$

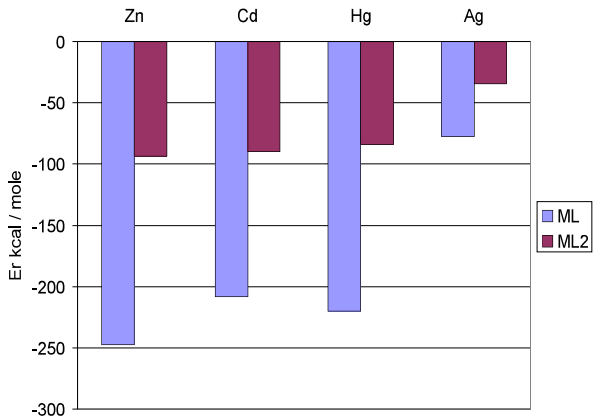


Figure 11 Representation of the calculated enthalpy by the coordination of 9AneS3.

The results of this calculation show that zinc forms stronger complexes with respect to Cd(II), Hg(II) and Ag(I) and, in this case, $Hg^{2+}$ shows an energy gain intermediate between $Zn^{2+}$ and $Cd^{2+}$. This trend does not follow the experimental enthalpy order in solution (see Table 1). The effect of solvent has therefore also taken into account. In the equation (2.16) and (2.17) the energies for the formation of the complexes with 9AneS3 are calculated considering the additional displacement of AN molecules.

$$M(AN)_{x(g)}^{n+} + 9AneS3_{(g)} \rightarrow M(AN)_{x-3}(9AneS3)_{(g)}^{n+} + 3AN_{(g)} \quad (2.16)$$

For Zn(II) and Cd(II) $x$ was considered equal to 6, for a comparison with structural solid state data [65], whereas for Ag(I), $x$ was shown to be equal 4 in AN solutions by reported studies [66].

$$M(AN)_{x-3}(9AneS3)_{(g)}^{n+} + 9AneS3_{(g)} \rightarrow M(9AneS3)_{2(g)}^{n+} + (x-3)AN_{(g)} \quad (2.17)$$

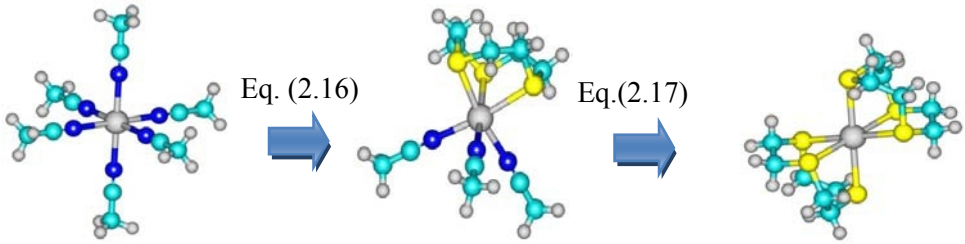


Figure 12 Structures of the starting, intermediate and final mercury complexes. Colors correspond to the following atoms: central gray = Hg, yellow = S, dark blue = N, blue = C and outer gray = H.

The complex $Hg(9AneS3)_2$ shows (Figure 12) a tetragonal elongation or compression of the structure from idealized octahedral geometry, as reflected in the literature [46].The distorted octahedral geometry illustrates the ability of the 9AneS3 ligand to force facial tridentate coordination on metal ions, such as Hg(II), that usually do not favor hexa coordination.

It is worthwhile to consider also the results in Figure 13 where the optimized structures of $[Zn(AN)_6]^{2+}$ and $[Zn(9AneS3)(AN)_3]^{2+}$ are displayed: they are in good agreement with the available [21] crystal structure.

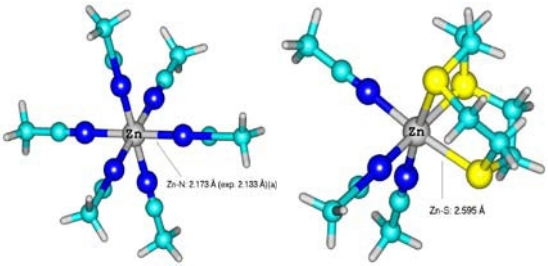


Figure 13 Structures of $[Zn(AN)_6]^{2+}$ and $[Zn(9AneS3)(AN)_3]^{2+}$. Colors correspond to the following atoms: central gray = Zn, yellow = S, dark blue = N, blue = C and outer gray = H.

The dissociation of first shell solvent molecules in vacuum can give positive values (Figure 14): this can depend on the calculation method, but the important point is to focus on the relative values. The reaction energy increases now in the order: silver < mercury < cadmium < zinc.

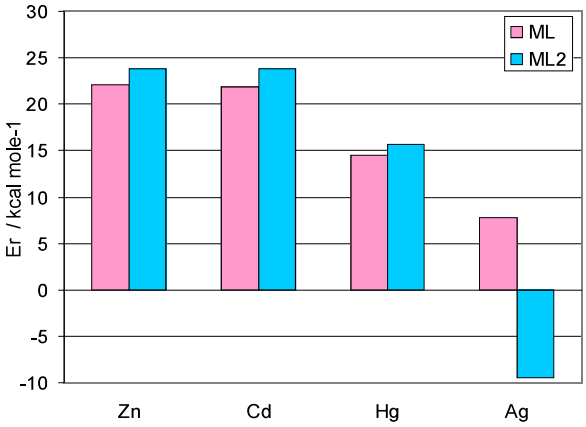


Figure 14 Energies of reactions 2.16 and 2.17 in vacuum including dissociation of first shell solvent molecules

When the energies are recalculated with the solvent modeled as polarizable continuum, the most favorable energies are obtained for mercury complexation. In addition, the relative values for the bipositive ions (Figure 15) indicate that zinc and cadmium are evidently better solvated than mercury, given the more positive reaction energy. The trend here reported agrees with the experimental enthalpy trends and from the sum of the results one can conclude that the selectivity is clearly due to solvent effects.

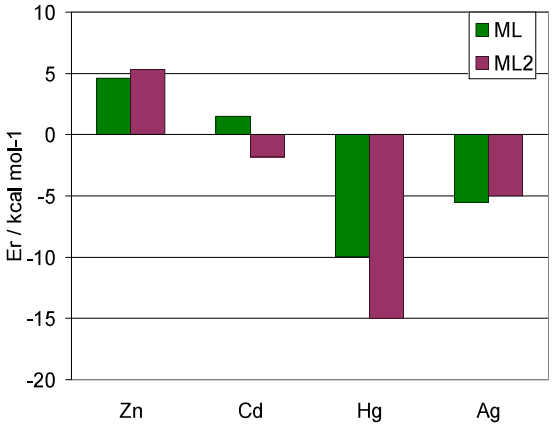


Figure 15 Energies of reactions 2.16 and 2.17 with the “bulk” solvent effect modeled as polarizable continuum.

This result, according with the experimental evidences, indicates that the preferential coordination of 9AneS3 to $Hg^{2+}$ with respect to $Zn^{2+}$ and $Cd^{2+}$ is originated by a combined coordination/solvation energetics rather than by an intrinsic higher affinity of $Hg^{2+}$ for this cyclic thioether.

### *2.1.3.3. Diethyl sulfide ($Et_2S$)*

Diethyl sulfide (Figure 1) has been investigated to obtain the energetic contribution of a single thioether group to the formation of the metal-ligand bond.

Both potentiometric and calorimetric measurements did not detect formation of Zn(II) and Cd(II) complexes with $Et_2S$, even at high metal to ligand ratios (1:5).

Therefore, this ligand forms complexes only with Ag(I) and Hg(II), of much lower stability than 9AneS, with much less favorable enthalpy values (Table 2). This can be explained because $Et_2S$ coordinates with single donor atom, and therefore, the value of the enthalpy could be comparable with the heat produced by the coordination between the metal and the first sulfur atom of the cyclic thioether. It is noticeable that the enthalpy value for the formation of the 1:1 species with Ag(I) and Hg(II) is around 1/3 of the value obtained for 9AneS3.

Table 2 The thermodynamic data for $Et_2S$ in AN.

| | **log β°** | **-ΔG° (kJ/mol)** | **-ΔH° (kJ/mol)** | **TΔS° (kJ/mol)** |
|---|---|---|---|---|
| **$Ag(Et2S)^+$** | 2.11 (±0.01) | 12.0 (±0.1) | 19.0 (±0.2) | -7.0 |
| **$Ag(Et2S)_2^+$** | 3.97 (±0.01) | 22.7 (±0.1) | 29.6 (±0.2) | -6.9 |
| **$Hg(Et2S)^{2+}$** | 10 (±1) | 57.1(±0.1) | 32.8 (±0.3) | 24.3 |
| **$Hg(Et2S)_2^{2+}$** | 15* | 89* | 65.2 (±0.4) | 23.8 |

* Estimated value from calorimetric data.

As far as Hg(II) is concerned, the polarographic analysis determines, for the range of concentration ($9.28 \cdot 10^{-3}$ M - $1.37 \cdot 10^{-4}$ M) studied, a constant half-wave potential value of +0.264 mV. Therefore, the formation of only 1:1 ML complex results with a value of logβ = 10 ± 1, despite in calorimetric experiments a weaker $ML_2$ complex is also detected (  ).

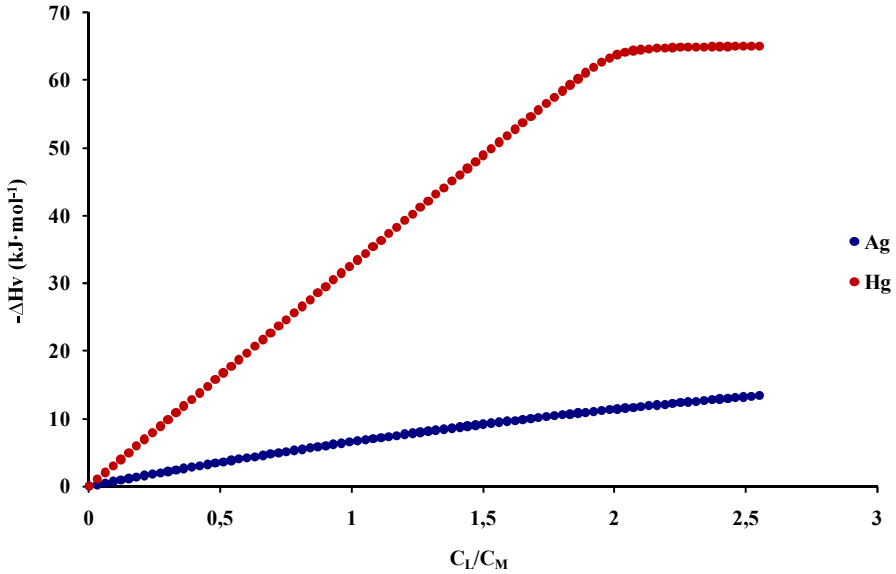


Figure 16 Calorimetric titrations for $Et_2S$ ($6 \cdot 10^{-2}$ M) with Ag(I) and Hg(II) ($5 \cdot 10^{-3}$ M) in AN.

### *2.1.3.4. 1,4,7,10-tetrathiacyclododecane (12AneS4)*

The 12AneS4 (Figure 1) is a cyclic tetridentate ligand, which presents a low solubility in AN (approximately 17 mM at 298 K); this was a limitation which prevented the possibility to obtain reliable calorimetry data given the sensibility of the Tronac instrument. Therefore, only stability constants have been determined for Ag(I), Zn(II) and Cd(II) by potentiometric method and for Hg (II) by polarographic method, which are reported in Table 3.

Table 3 The thermodynamic data for 12AneS4 in AN.

| | log β | -ΔG° (kJ/mol) |
|---|---|---|
| **Ag(12AneS4)$^{+}$** | 6.07 (±0.01) | 34.63 (±0.03) |
| **Zn(12AneS4)$^{2+}$** | 3.12 (±0.01) | 17.83 (±0.08) |
| **Cd(12AneS4)$^{2+}$** | 3.00 (±0.04) | 17.1 (±0.2) |
| **Cd(12AneS4)2$^{2+}$** | 6.69 (±0.01) | 38.21 (±0.04) |
| **Hg(12AneS4)$^{2+}$** | 15.6 (±0.3) | 89.0 (±0.1) |

The competitive potentiometric titration data, reported in Figure 17, show that the 12AneS4 forms complexes with all metal studied.

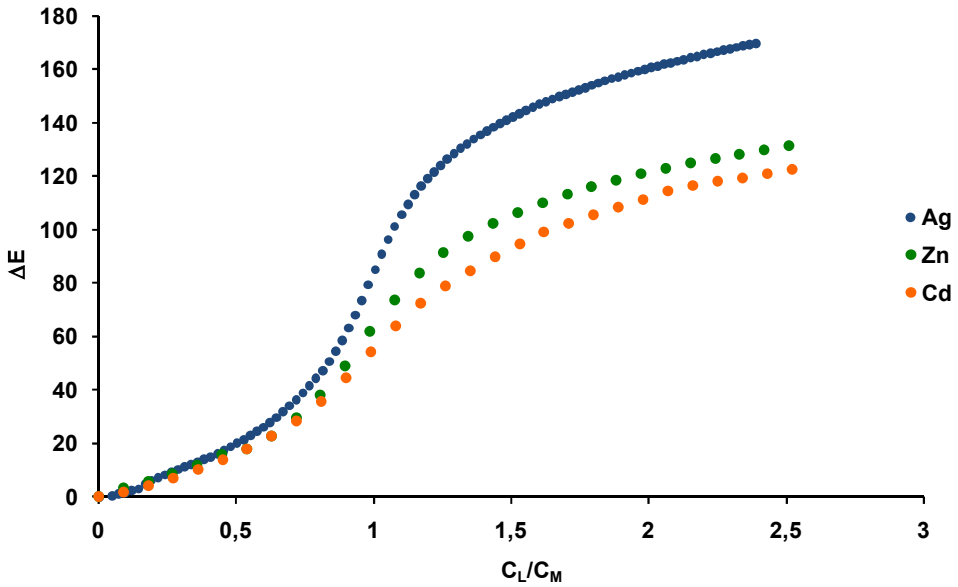


Figure 17 Competitive potentiometric titration for 12AneS4 ($1.25 \cdot 10^{-3}$ M). Concentration of metals are Ag(I) = $1 \cdot 10^{-3}$ M (without the presence of competing metal), Ag(I) = $1 \cdot 10^{-3}$ M (with the presence of competing metal) and Zn(II) and Cd(II) = $4 \cdot 10^{-3}$ M in AN.

Anyway, the minimization of data, show that the best fit was achieved when the formation of a single complex 1:1 is considered for Ag(I) and Zn(II), with a stability comparable to the respective tridentate ligand complex. This could indicate that in these ML complexes the quatridentate ligand is coordinated with only three of the S-donor atoms.

However, for Cd(II), formation of two complexes (ML and $ML_2$) has been observed. This may be due to the ionic size cadmium which is larger, and therefore allows the coordination of a second ligand molecule. Again, the values of the stability constants are similar to those obtained for 9AneS3.

The results for Hg (II) with this ligand, are based only on the polarographic data, for the reasons discussed above. The results of the polarograms show, for the range of concentration ($1.01 \cdot 10^{-2}$ M – $2.51 \cdot 10^{-4}$ M) studied, a constant half-wave potential value of +0.121 mV. Therefore, the formation of ML complex with a value of $\log\beta = 15.6 \pm 0.3$ is indicated. Again the ligand is much more selective for Hg(II), the value of the constant being similar to the estimated value for ML formation with 9AneS3 this may be due to several factors such as a non complete binding or to a non-optimal fit of the cation in the ligand structure.

### *2.1.3.5. 1,4,8,11-tetrathiacyclotetradecane (14AneS4)*

The 14AneS4 (Figure 1) is a tetradentate S-donor ligand with a larger ring cavity with respect to the other ligands presented above.

The experimental data show that Zn(II) and Cd(II) complexes are not formed with 14AneS4. The whole of thermodynamic data obtained for Ag(I) and Hg(II) are reported in Table 4.

Table 4 The thermodynamic data for 14AneS4 in AN.

| | log β | -ΔG° (kJ/mol) | -ΔH° (kJ/mol) | TΔS° (kJ/mol) |
|---|---|---|---|---|
| **$Ag(14AneS4)^{+}$** | 3.82 (±0.02) | 21.8 (±0.1) | 57 (±2) | -35.2 |
| **$Hg(14AneS4)^{2+}$** | 15.8 (±0.6) | 90 (±0.1) | 88 (±2) | 2 |
| **$Hg(14AneS4)_2^{2+}$** | 21* | 121* | 116 (±3) | 5 |

* Estimated value from calorimetric data.

In the case of Hg(II) the polarographic analysis determines, for the range of concentration ($1.19\cdot10^{-3}$ M - $1.85\cdot10^{-4}$ M) studied, a constant half-wave potential value of +0.115 mV. Therefore, the formation of ML complex with a value of logβ = 15.8 ± 0.6 is evaluated, despite in calorimetric experiments is also appreciated the $ML_2$ complex formation with a smaller constant, $\log K_2 = 5.2$ (Figure 18).

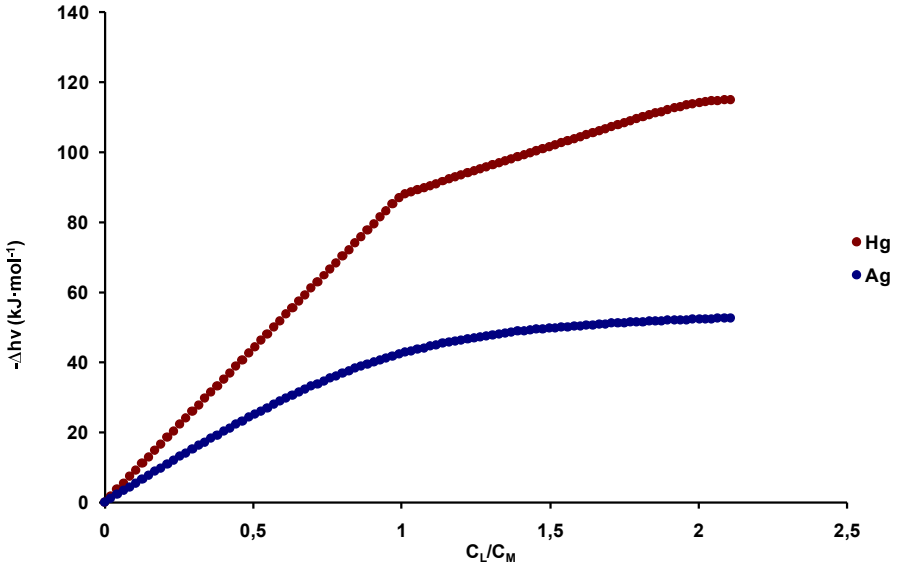


Figure 18 Calorimetric titrations for Hg(II) and Ag(I) ($2\cdot10^{-3}$ M) with 14AneS4 ($1.68\cdot10^{-2}$ M) in AN.

The behavior of Hg(II) is similar in relation to the formation of ML complex for this ligand and the 9AneS3, but the reaction is more exothermic when tridentate ligand is considered, indicating that the interaction is weaker in 14AneS4, probably because of the larger distance between the thioether groups which prevents an optimal fit into the cavity.

### *2.1.3.6. Dimethylsulfoxide as solvent*

The study has also been extended to the more coordinating solvent DMSO. The calorimetric data for Ag(I) and Hg(II) with the ligands 9AneS3, $Et_2S$ and 14AneS4 are presented in Figure 19 where it emerges that the complexes formed by all tree ligands present a lower heat evolved in DMSO with respect to AN (see also Figure 10 and 11 for a comparasion): this can be due to a higher metal solvation in DMSO [64]. For Zn(II) and Cd(II) no interaction is observed. This can be explained by observing the thermodynamic transfer parameters of these ions from AN to DMSO, which are largely negative (the $\Delta H^{tr}_{AN \rightarrow DMSO}$ for $Ag^+$, $Zn^{2+}$, $Cd^{2+}$ and $Hg^{2+}$ are -10, -80, -78 and -70 $kJ \cdot mol^{-1}$ respectively) [64], and evidently prevent the formation of Zn(II) and Cd(II) complexes in our experimental conditions. Therefore, thermodynamic values in DMSO are reported for Ag(I), and for Hg(II) in the Table 5 and Table 6, respectively.

Table 5 The thermodynamic data for Ag(I) with the ligands reported in DMSO.

| | **log β** | **-ΔG° (kJ/mol)** | **-ΔH° (kJ/mol)** | **TΔS° (kJ/mol)** |
|---|---|---|---|---|
| **$Ag(9AneS3)^+$** | 4.95(±0.01) | 28.3 (±0.1) | 56 (±1) | -27.7 |
| **$Ag(9AneS3)_2^+$** | 7.82 (±0.01) | 44.6 (±0.1) | 84 (±3) | -39.4 |
| **$Ag(14AneS4)^+$** | 3.09 (±0.01) | 17.6 (±0.1) | 21.3(±0.2) | -3.7 |
| **$Ag(Et_2S)^+$** | 2.31 (±0.01) | 13.2 (±0.1) | 17 (±1) | -3.8 |
| **$Ag(Et_2S)_2^+$** | 3.29 (±0.01) | 18.8 (±0.2) | 34 (±1) | -15.2 |

Table 6 The thermodynamic data for Hg(II) with the ligands reported in DMSO.

| | log β | -ΔG° (kJ/mol) | -ΔH° (kJ/mol) | TΔS° (kJ/mol) |
|---|---|---|---|---|
| **$Hg(9AneS3)^{2+}$** | 5.7 (±0.3) | 33 (±1) | 39 (±1) | -6 |
| **$Hg(9AneS3)_2^{2+}$** | 9.9 (±0.3) | 55 (±1) | 77 (±2) | -22 |
| **$Hg(14AneS4)^{2+}$** | 3.5 (±0.3) | 20 (±1) | 9.0 (±0.1) | 11 |
| **$Hg(14AneS4)_2^{2+}$** | 5.6 (±0.3) | 32 (±1) | 11.3 (±0.1) | 20.7 |
| **$Hg(Et_2S)^{2+}$** | 2.3 (±0.3) | 13 (±1) | 17(±1) | -4 |
| **$Hg(Et_2S)_2^{2+}$** | 3.3 (±0.3) | 19 (±1) | 42 (±1) | -23 |

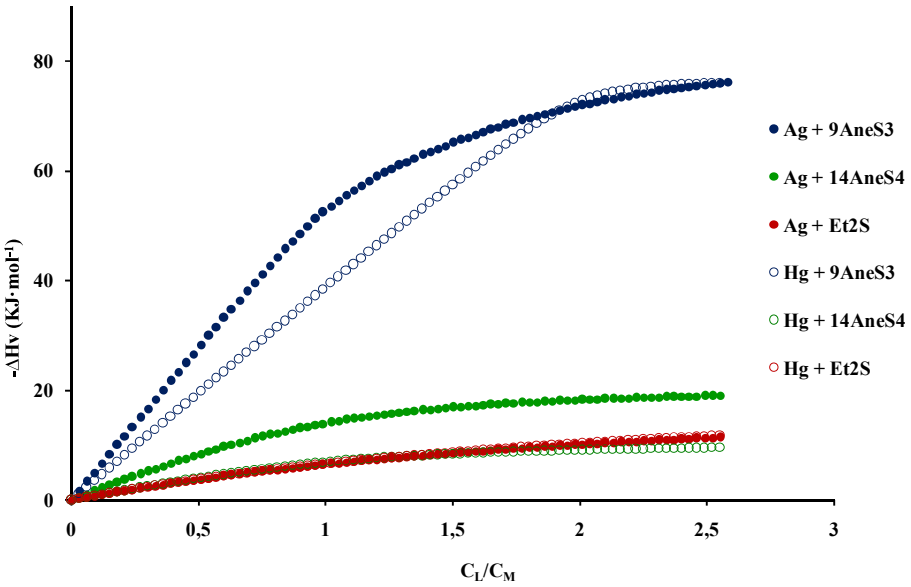


Figure 19 Calorimetric titrations for Ag(I) ($5\cdot10^{-3}$ M) and Hg(II) ($5\cdot10^{-3}$ M) with the ligands reported ($6\cdot10^{-2}$ M) in DMSO.

Only for Hg in DMSO (Table 6), both logβ and enthalpy values were obtained from calorimetric data. In the case of 14AneS4, a positive entropy can be appreciated. This can be because the 14AneS4 has a larger ring, therefore the second donor atom is coordinated with more difficulty by the increase in the length of the chain. In other words, the loss of molecules by the metal desolvation is probably greater than the number of S-donors to

coordinate Hg(II) because of the structural constraints in the tetradentate ligand, and consequently the contribution of the entropy of the complex is greater.

Finally, the same theoretical calculations previously employed in AN (see section 2.1.2.5), have been used to obtain indications about the effect of solvent in the coordination of tridentate ligand 9AneS3. When the energies are recalculated for mercury and silver in DMSO, reversed reaction energies are obtained with respect to AN (Figure 20). This can be explained because Hg(II) is more strongly solvated than Ag(I) by DMSO. This is in agreement with the observed experimental enthalpy values (Table 5 and Table 6) and confirms that (the small) preference of thioethers for binding Hg(II) with respect to Ag(I) in DMSO is of entropic origin.

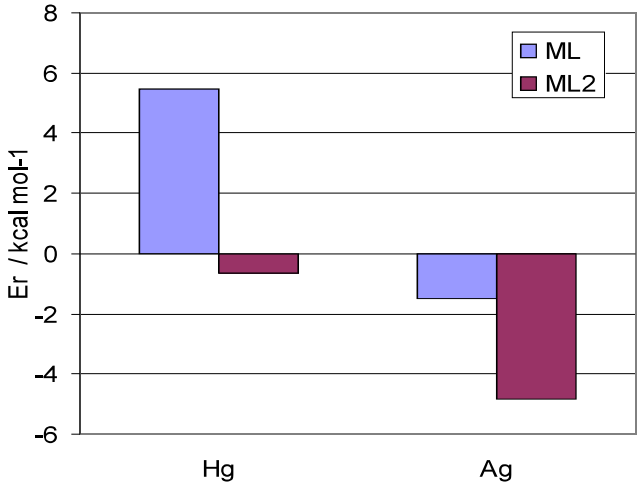


Figure 20 Representation of the calculated enthalpy by combined coordination/solvation energetic for 9AneS3 in DMSO.

## 2.2. Studies and applications of Hg and 9AneS3 complex formation using liquid-Liquid Distribution Processes

### *2.2.1. Introduction*

Separation processes are used in many industrials activities. For many companies, these processes involve the production of specific materials. On the other hand, in the environmental field, the principal objective of the separation process is the recovery, disposal and/or treatment of certain pollutants. For reasons considered above, it is known the separation processes to have great economic and social impact.

There are multiple separation techniques taking into account that the separation process can be divided into equilibrium processes (evaporation, desorption, adsorption, ion exchange, solvent extraction, reverse osmosis, etc...) processes controlled by the speed (thermal diffusion, diffusion gas, dialysis, electrophoresis, reverse osmosis, etc..) and mechanical separation processes (filtration, sedimentation, centrifugation, precipitation, etc.) [29].

Solvent extraction has become a very powerful method of separation for various reasons, in particular, it is very simple, rapid, selective and sensitive. This method does not need sophisticated instrumentation and can use a good array of ligands with a variety of functional groups containing donor elements, i.e, to extract metal ions. Solvent extraction of metals is dominated by formation of metal compounds.

During the past decades, much attention has been paid to chemical separation techniques and the selective determination of heavy metals by solvent extraction. The removal of these trace heavy metal ions is reported by several solvent extraction methods [67, 68]. Specifically, the assay of mercury compounds has been a challenging problem, not only due to their widespread agricultural and industrial use, but also because of their hazardous effects on human health, as explained in section 1.1. For this reason, the development of new procedures for selective separation and removal of mercury for environmental remediation has remained an important objective [69] In this context, related studies of

liquid-liquid systems have been carried out in the present thesis including thermodynamic characterization and analytical applications of mercury by pre-concentration using adsorption on particular solid support.

### *2.2.2. Experimental*

#### *2.2.2.1. Chemicals*

Nitrate stock solutions of Zn(II), Cd(II), Hg(II) ions were prepared by dissolving in water weighed amounts of the adducts and their concentrations were checked by back titration with EDTA. The stock solutions of 9AneS3 were prepared by dissolving in organic solvent (dodecane and hexane).

#### *2.2.2.2. Liquid-liquid extraction*

In an operation of liquid-liquid extraction the solvent A containing the components to separate, called *feed*, is put in contact with a solvent B immiscible with A. Figure 21 shows a diagram of the currents involved in the operation. The solution of B with the components separated is called *extract*. The solution of A after the extraction is called *refined*. Eventually, the refined phase can be concentrated and recycled for successive extractions in order to eliminate the residual components to separate.

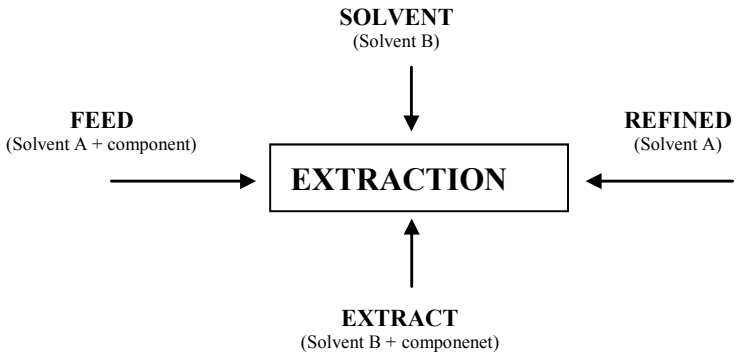


Figure 21 Idealized scheme of operation of liquid-liquid extraction

This simple type of extraction is very useful to study the different parameters that influence the separation process. Some of these are: pH, analyte concentration, the concentration of extractant, temperature, effect of co-solvents.

In our experiments, equal volumes of the aqueous solution of the metal nitrates and an organic solvent (dodecane or hexane) were mixed in glass tubes and shaked for 15 min. at 50 rpm at room constant temperature (~22 °C).

Afterwards, the dispersion was centrifuged for an easier and faster separation of the phases (for 1 min at 2000 rpm) (Figure 22).

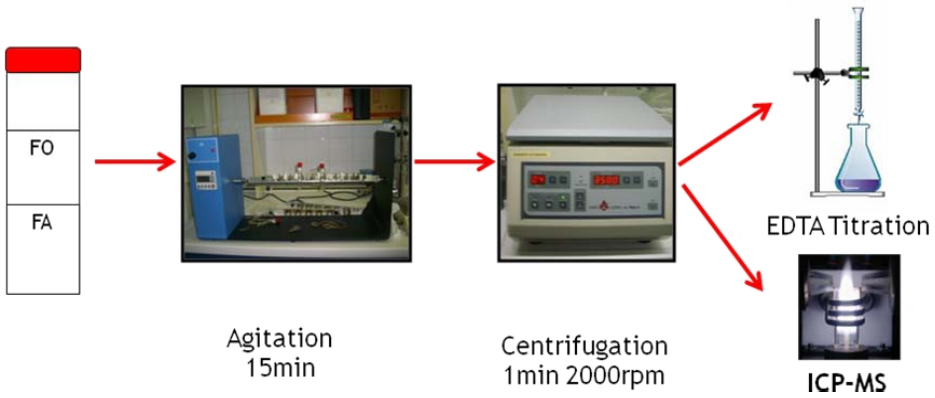


Figure 22 Scheme the process of Liquid-Liquid Extraction. FO: organic phase. FA: aqueous phase.

The determination of the concentration of mercury in aqueous phase was performed by back-titration with EDTA [55] and the determination of the amount of sulfur present in the aqueous phase after reaching the liquid-liquid equilibrium was carried out by an ICP-MS analytical method.

The metal extraction percentage was calculated as follows:

$$E(\%) = 100\frac{[M]_i - [M]_{aq}}{[M]_i} \tag{2.18}$$

Where $[M]_i$ and $[M]_{aq}$ in M, are the initial and equilibrium total metal concentration in the aqueous phase, respectively.

### *2.2.2.3. Analytical test to verify the formation and stability of aqueous Hg(II)-9AneS3 complex*

In order to verify both the formation and stability of Hg(II)-9AneS3 complex in aqueous solution, the following test were carried out:

- Test 1. Few mg of 9AneS3 was deposit in two vials. In one, 5 mL of water were added and 5 mL of a solution of $Hg(NO_3)_2$ were added to the other one. Then the two solutions were sonicated. The results showed that the 9AneS3 of the vial containing only water had not been dissolved, while the 9AneS3 of the vial containing a solution of $Hg(NO_3)_2$ had completely dissolved, indicating thus the possible formation of Hg(II)-9AneS3 complexes.

- Test 2. An aqueous solution containing only Hg(II) was agitated with a hexane solution of 9AneS3. After equilibrium, the aqueous solution was analyzed by using the method of back titration with EDTA that determined a portion of the initial Hg(II) which corresponds to the aqueous Hg(II) non complexed by 9AneS3 ligand.

- Test 3. Finally, $H_2O_2$ was added to the dissolved sample obtained from Test 2 in order to break the complex formed between Hg and 9AneS3. A posterior EDTA back titration revealed all Hg(II) to be non complexed, verifying thus the corresponding destruction of the previously formed complex.

### *2.2.2.4. Adsorption on cellulose and polyurethane sponge*

The goal is to impregnate the sponge with the ligand and after passing a solution containing the metal. This technique allows concentrating the sample and allows determining the concentration of metal by XRF easily.

The experiment proceeded as follows:

1. Cleaning of the sponge with 20 mL of water and 10 mL of hexane.
2. Drying the sponge to constant weight in the oven.
3. Measuring the metal content of the sponge with FP-XRF.
4. Impregnation of the sponge with 20 mL of a 0,251 mM solution of 9AneS3. The sponge is placed in a 10 mL syringe and 5mL are taken each time.
5. Drying the sponge to constant weight in the oven.
6. Measuring the metal content of the sponge with FP-XRF.
7. Following the impregnation at procedure 4, using in this case 20 mL of $Hg(NO_3)_2$ solution (0,03 mM).
8. Drying in a desiccator to constant weight.
9. Measuring the metal content of the sponge with FP-XRF.

### *2.2.2.5. Analytical methods to determine metal concentration*

#### *2.2.2.5.1. Determination with EDTA. Back titration*

The back titration is useful for analysis of cations that form very stable complexes with EDTA and for which there is available an adequate indicator [55]. The back titration involves adding to the sample a known amount of EDTA. Subsequently, the excess of EDTA is titrated with a solution of $ZnCl_2$, using hexamine buffer at pH = 6 and Xylenol Orange as indicator. In our case, the concentration of mercury before and after the liquid-liquid extraction has been determined by this method. This is possible because the HgEDTA complex is more stable ($\log\beta_1 = 21.5$) [70] than the ZnEDTA complex ($\log\beta_1 = 16,26$) [71] to avoid displacement of the Hg(II) ion and free EDTA is only complexed. Corresponding process equations (charges omitted) are:

$$Hg + EDTA \rightarrow HgEDTA + EDTA_{(ecess)} \tag{2.19}$$

$$EDTA_{(ecess)} + Zn \rightarrow ZnEDTA \tag{2.20}$$

### *2.2.2.5.2. Inductively coupled plasma mass spectrometry (ICP-MS)*

The radiofrequency generator of solid state of the ExCell PQ model [72] operates at 27.12 MHz and can generate a minimum power of 2000 W. Normally, neutralization is carried out using a concentric nebulizer (Meinhard). The spray chamber is conical ball impact a Peltier cooled to a temperature of 4 ºC, controlled by software. The diameter of injector is 1.5 mm. The diameters of the sampling cone and skimmer, made of Ni, is 1 and 0.7 mm respectively.

At pressures of $6x10^{-7}$ mbar, the flow of ions is guided through the lens system optimized for a potential series, targeted to the quadrupole, where the ions are discriminated by electric and magnetic field generated in the region bounded by the quadrupole reconstructed using molybdenum. Once discriminated, the ions are directed toward the detector. This detector is composed by a system of discrete dynodes electron multiplication. The dynodes are inside a glass tube of 1 mm internal diameter, with an inert coating and operation similar to a photomultiplier tube. The combination of the team autosampler and peristaltic pump is governed by the Plasmalab ® software (version 1.5)

The liquid samples introduced into the instrument must contain, as a rule, less than 0.2% of dissolved solids for minimized the deposition on the cones (sampling and skimmer) that includes the interface between the torch and the lens system. Otherwise, the obturation of the passage of ions through these cones will be favored. On the other hand, the use of organic solvents requires adjustment of the conditions for maintaining the plasma. Finally, the acidity of the samples should be limited to 2% ($HNO_3$ and HCl) and 1% $H_2SO_4$, since higher contents can erode the interface.

The calibration is performed using standards prepared from monoelemental and commercial multielement stock solutions using matrices resulting from the treatment of the samples for the matrix adjustment. Different internal standards for correction of instrumental and matrix effects were used, with Li and Sc for low mass, Y, In, Rh or

Ga for intermediate mass and Bi or Tl for high mass [73]. In our case, we have used an internal standard with Rh, In, Ga (5 ppb of each). The majority of selected isotopes analytes of interest are free of polyatomic isobaric. The analytical determinations were performed in triplicate including blank procedure, reagents and containers.

The quality of calibration has been verified using external control samples, evaluating both the calibration and reproducibility of the samples. Instrumental parameters and the masses used for each element selected characteristics are shown in Table 7 and Table 8 respectively.

Table 7 Instrumental operating conditions. ICP-MS ThermoElemental Pq ExCell.

| PARAMETER | VALUE |
|---|---|
| Generator power | 1350 W |
| Generator frequency | 27.15 MHz |
| Integration time | 120 s |
| Ar flow (plasma) | 13-15 $L \cdot min^{-1}$ |
| Ar flow (auxiliary) | 0.90-0.95 $L \cdot min^{-1}$ |
| Nebulizer flow | 0.85-0.95 $L \cdot min^{-1}$ |
| Peristaltic pump flow | 2 $mL \cdot min^{-1}$ |
| Acquisition time | 35-55 s |
| Wash time | 85-65 s ($HNO_3$ 1%) |
| mode | Peak jump y scan |
| Mass channels | 10 |
| sweeps | 100 |
| Time for mass | 10000 μs |

Table 8 Summary of masses employed and polyatomic and isobaric interferences observed.

| ELEMENT | ISOTOPES | Isobaric/Polyatomic INTERFERENCES |
|---|---|---|
| Hg | 200/202 | memory effect |
| Zn | 64/66/68 | 64Ni / 40Ar, 14N |
| Cd | 111 | 95Mo,16O+ |

### *2.2.2.5.3. Field Portable X-ray Fluorescence (FP-XRF)*

The technique of X-ray fluorescence has been used, along the present study to determine the amount of mercury in different stages of adsorption on cellulose sponges.

X-ray fluorescence is based on irradiation of the sample with X-ray of energy high enough to penetrate the interior of the atom and move an electron from the orbital K and L near the nucleus, causing the expulsion of an electron and ionizing the atom. Subsequently, this vacancy is filled by electrons from higher energy orbitals to stabilize the atom. During this process, energy is released as X-rays which are determined by appropriate instrumentation [74-76].

For the measurement of X-ray fluorescence analyzer was used portable X-ray fluorescence (FP-XRF), Alpha model 6500 (Figure 23), equipped with a generator of ionizing radiation comprising X-ray tube with a tungsten cathode a silver anode, which operates within the range of 10-40 keV and 10-50 μA of current. A diode detector that works If PiN <230 eV FWHM at 5.95 keV (Ka line of magnesium) is used. Standardization was used for a reference steel (AISI316), and with respect to calibration, it was verified using a certified reference material (NIST 2710). The team is controlled by Innov-X software.

Figure 23 X-ray fluorescence (FP-XRF), Alpha model 6500

### *2.2.3. Results and discussion*

#### *2.2.3.1. Liquid-liquid extraction*

This thesis presents the study of the complex formation between mercury ions in aqueous phase and the macrocycle 9AneS3 dissolved in hexane as complexing agent. The motivations of this study have been widely explained in section 1.

As detailed in the experimental section (2.2.2) the formation of Hg(II)-9AneS3 stable complexes in aqueous solution was verified. This fact produces the extraction of the related amount of the ligand 9AneS3 from the organic to the aqueous phase. Thus, in this case, the distribution process between the two phases corresponds to the ligand 9AneS3.

Therefore, the equilibrium reaction of the process occurring can be expressed as:

$$Hg^{+2}_{(aq)} + n9AneS3_{(org)} \leftrightarrows Hg(9AneS3)^{+2}_{n\,(aq)} \tag{2.21}$$

Therefore and to express the experimental data, we use the term *formation percentage* corresponding to the complexation of mercury in aqueous phase.

The distribution coefficient of the ligand (D) is defined by:

$$D = \frac{[L]_{(aq)}}{[L]_{(org)}} = \frac{[Hg(9AneS3)^{2+}_{n}]_{(aq)}}{[9sneS3]_{(org)}} \tag{2.22}$$

where $[L]_{(aq)}$ and $[L]_{(org)}$ (where $[L]_{(org)} = [L]_{tot} - [L]_{(aq)}$) are the total concentration of ligand in aqueous and organic phase, respectively.

In the case of metal, the coefficient $F_M$ (formation coefficient) is defined as:

$$F_M = \frac{[M]_{(compl)}}{[M]_{(free)}} = \frac{[Hg(9AneS3)_n^{2+}]_{(aq)}}{[Hg]_{(aq)}} \tag{2.23}$$

where $[M]_{(compl)}$ and $[M]_{(free)}$ are the concentration of complexed and free mercury, respectively, in the aqueous phase.

To characterize this process, it is important to study different parameters that affect the process at equilibrium. Thus, some basic parameters have been considered for this characterization: the solvent, pH, temperature and concentrations of analyte (Hg (II)) and ligand (9AneS3).

#### *2.2.3.1.1. Effect of the Solvent selected*

We have studied the effect of two solvents used in extraction processes, dodecane [77] and hexane [78].

In all cases, experiments were carried out with an initial solution of Hg $(NO_3)_2$ of 1.5 mM in the aqueous phase. This has been in contact with the organic phase for two different ligand concentrations (1.5 and 3 mM). The results, performed in duplicate, are presented in the following Table 9.

Table 9 Formation percentage for Hg (1.5 mM and 3 mM) in hexane and dodecane.

| **initial concentration of Hg (mM)** | **% formation HEXANE** | **% formation DODECANE** |
|---|---|---|
| 1.5 | 55 | 71 |
| 3 | 100 | 97 |

The results show a high formation percentage in both cases, however, for hexane, when the ligand concentration in the organic phase is twice the metal in the aqueous phase, a total formation of complex was obtained. Hexane, has a boiling point, density and viscosity lower than the dodecane, allowing easier operations [44]. Therefore, the hexane solvent has been selected for the rest of the experiments.

#### *2.2.3.1.2. Effect of pH*

The experiments at different pH were carried out with an initial solution of $Hg(NO_3)_2$ of 1.5 mM and a 3.5 mM solution 9AneS3. The extractions were performed in a pH range of 0.44 to 11.42 adjusted appropriate additions of either with $HNO_3$ or NaOH solutions.

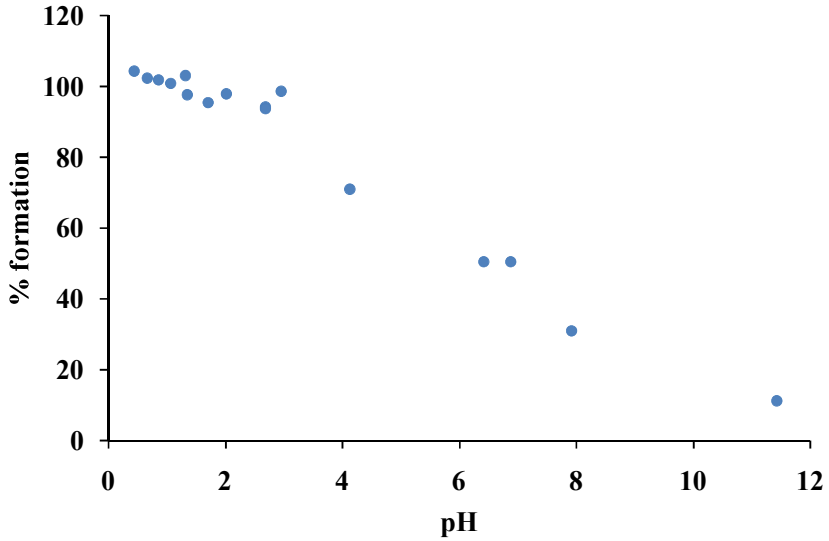


Figure 24 Effect of pH in the % formation.

The representation of the formation percentages depending on the initial pH of loading solution (Figure 24) shows that the total complexation of mercury is obtained at acid pH between 0.44 and 3, while at pH above 3 decreases the efficiency of complexation. Therefore, the optimal range for the process is pH 0.5 - 3. In our case, we chose a pH = 3,

because in the working conditions the concentration of mercury nitrate salt has a pH 3 without need to be further modification.

The observed decrease with pH of the Hg(II)-9AneS3 complex formation can be interpreted by the related hydrolysis of Hg(II). Thus, competition of $OH^-$ ions with 9AneS3 hinders the related complex formation

### *2.2.3.1.3. Effect of Temperature*

Experiments at different temperatures were performed in an incubator that can regulate the temperature between 25 and 49 $^oC$. Two replicates were prepared at three temperatures: 25, 40 and 49 $^oC$. Both initial concentrations of mercury and 9AneS3 were 1.5 mM. In these initial conditions and at room temperature (20-22 °C) complex formation resulted to be 57%.

The results shows the temperature does not affect the complexation of mercury with 9AneS3 within the studied range 25-49 $^oC$. This may suggest that associated formation enthalpy for this complex is low.

### *2.2.3.1.4. Effect of concentration of Hg and 9AneS3*

A series of experiments were conducted. First, by varying the concentration of 9AneS3 in hexane with an excess of mercury in the aqueous phase over the 9AneS3 concentration. In this case, three sets of extractions were carried out with initial concentrations of $Hg(NO_3)_2$: 0.7 mM, 1 mM and 1.5 mM respectively. For the different extractions metal concentrations, the ligand 9AneS3 concentration was varied as 0.49 mM, 1.00 mM, 1.49 mM, 2.02 mM, 2.54 mM, 3.03 mM and 3.51 mM in hexane. In the case of the $Hg(NO_3)_2$ concentration of 1.5 mM, the 9AneS3 range was extended to 6 mM, 10 mM, 15 mM and 20 mM.

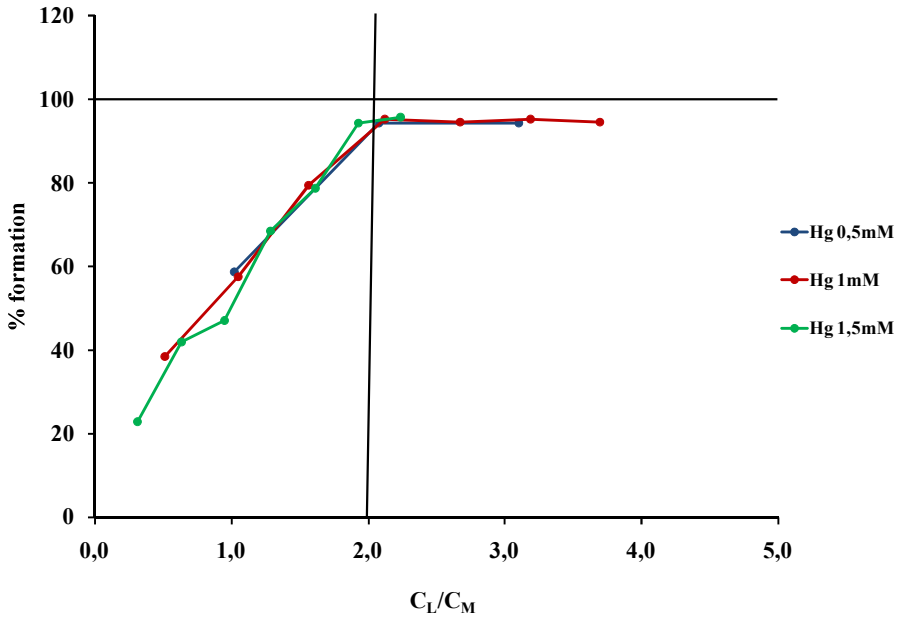


Figure 25 Plot of the % formation of mercury vs. the ratio $C_L/C_M$

The Figure 25 shows the % formation vs. the ratio $C_L/C_M$, where $C_L$ is the concentration of 9AneS3 total and $C_M$ is the initial mercury concentration. This graphic shows that in all three cases, the maximum extraction is obtained when the ratio $C_L/C_M$ is equal to 2. The obtained data reveal the main stoichiometry of the complex formation following equation 2.21 to be Hg(II):$(9AneS3)_2$.

A second set of experiments were carried out by varying the concentration of mercury with an excess of 9AneS3 in the organic phase. In this case, two initial solutions of 1 mM and 1.5 mM of 9AneS3 were prepared. A group of solutions between 0.06 mM and 0.8 mM were used for extractions. In this case, EDTA titrations showed that all the mercury present in the aqueous phase was complexed with the 9AneS3. This is a clear consequence of the stability of the metal complex formation in aqueous phase.

In order to carry out a more accurate identification of the formed metal complexes and to quantify the related stability of the species formed, a numerical treatment of the experimental data was carried out by using the LETAGROP-DISTR program. In this concern and to directly ascertain the observed distribution of the ligand 9AneS3, determination of the amount of sulfur present in the aqueous phase after reaching the liquid-liquid equilibrium was carried out by an ICP-MS analytical method. Thus, quantitative distribution of 9AneS3 in the aqueous phase was attained.

#### *2.2.3.2. Determination of complex formation constants in aqueous solution from two phases experimental data*

Analysis of the experimental data obtained in the distribution equilibrium studies were evaluated using the computer program LETAGROP-DISTR [79]. This program searches for the best equilibrium constant that minimized the error squares sum, defined by:

$$U = \sum \left(logD_{exp} - logD_{calc}\right)^2 \tag{2.24}$$

Where $D_{exp}$ is the distribution coefficient determined experimentally and $D_{calc}$ is the value calculated by the program. This program also calculates the standard deviation σ(logD) defined by:

$$\sigma(logD) = \sqrt{\frac{U}{N_P}} \tag{2.25}$$

Where $N_P$ is the number of experimental points.

Analysis of solvent extraction data by LETAGROP-DISTR have shown the formation of 1:2 and in less extent 1:3 of Hg(II):9AneS3 aqueous complexes.

Table 10 Stability constant of the Hg-9AneS3 complex in water and DMSO.

| COMPLEXES Hg(II):9AneS3 | logβ (Aqueous Solution) | logβ (DMSO Solution) |
|---|---|---|
| 1:1 | ND | 5.7 (±0.3) |
| 1:2 | 8.9 (±0.5) | 9.9 (±0.3) |
| 1:3 | 11.1 (±0.4) | ND |

Comparison of the obtained results with those previously observed from results on thermodynamic study in DMSO (section 2.1.3.6) a lower stability the Hg-9AneS3 complexes in water with respect to DMSO is observed. Observing the thermodynamic transfer parameters of these ions from water to DMSO, which is positive (the $\Delta H^{tr}_{W \rightarrow DMSO}$ for $Hg^{2+}$ is 78 kJ·mol$^{-1}$) [64], would be expected a lower stability in DMSO, due to a higher Hg(II) solvation in DMSO [64]. However, this slightly less stability constant in water could be explained by a higher ligand solvation in water with respect to DMSO.

### *2.2.3.3. Application of the Hg(II)-9AneS3 complexes to the determination of small amounts of Hg(II). Use of selective adsorption on cellulose and polyethylene sponge*

A study on pre-concentration of mercury by adsorption on solid support was carried out with two types of commonly used commercial sponges: cellulose (CS) and polyurethane (PS) sponge. Experiments have been performed using the procedure explained in section 2.2.2.1.2.

The efficiency of pre-concentration in a sponge is defined as in equation (2.26):

$$preconcentration\ factor = \frac{ppm_{Hg}(sponge)}{ppm_{Hg}(solution)} \tag{2.26}$$

The results are shown in Table 11.

Table 11 Hg values (ppm) obtained with FP-XRF and the pre-concentration degree in two types of sponges: CS (Cellulose), PS (Polyurethane). "Background" sponges were not impregnated with 9AneS3.

| | **Average [Hg] (ppm)** | **Pre-concentration factor** |
|---|---|---|
| CS Background | 163 ± 21 | 26 |
| CS sample | 289 ± 16 | 46 |
| PS Background | 92 ± 11 | 15 |
| PS sample | 72 ± 7 | 11 |

The mercury complex formation reported here have been applied to determine traces of Hg(II) in aqueous solutions. The results showed a pre-concentration system including a 9AneS3 impregnated cellulose sponge provides more than one order of magnitude (40 to 50 fold) on Hg concentration, in contrast to the polyurethane foam that is not effective in our system. This may be due to the higher polarity of the cellulose material that facilitates the interaction with the Hg(II)-9AneS3 complexes at the sponge.

In addition it clearly emerges the effect of ligand by comparing the data of the background samples and impregnated ones. Especially in the case of Cellulose sponge, there is an increase of the pre-concentration factor close to 100%.

# 3. Constants of formation of lanthanide with BTPA in AN

## 3.1. Introduction

Lanthanide compounds have been extensively used in the last decades as luminescent chemosensors, for medical diagnostics and optical cell imaging, contrast reagents for magnetic resonance imaging, shift reagents for NMR spectroscopy, as well as for applications in fundamental and applied science such as organic synthesis, bioorganic chemistry, catalysis. These applications were favoured by the increased knowledge of fundamental properties (electronic, spectroscopic, thermodynamic, magnetic, structural) of the elements, achieved as a consequence of the rapid development of academic studies on the lanthanide coordination chemistry during the last three decades. In addition, $Ln^{3+}$ show chemical properties very similar to those of actinides(III) ($An^{3+}$). This chemical similitude is a challenging problem in the separation of $An^{3+}$ from excess of $Ln^{3+}$ in the nuclear waste treatments [80].

As common property the trivalent lanthanide ions [81] are hard species. Hardness increases somewhat with higher atomic number. Moving from left to right across the period (increasing atomic number), the radius of each $Ln^{3+}$ ion steadily decreases. This is referred to as 'lanthanide contraction'. They are typical hard Lewis acids and the bonding in their complexes is electrostatic and non-directional. As a result, steric factors govern the coordination geometry of lanthanide complexes. Coordination numbers are generally high (greater than 6, usually 8 or 9 or as high as 12) and coordination geometries are often irregular. Low coordination numbers can be achieved with very bulky ligands [82].

The unusual spectroscopic properties of the Ln(III) cations results from shielding of the 4f orbitals by the filled $5s^2$ and $5p^6$ sub-shells. For example, each of the elements have very characteristic and very narrow emission bands, mostly in the visible and near infrared range. Additionally, these f-f transitions are parity (and sometimes also spin) forbidden, resulting in very long lived excited states, with typical luminescence

lifetimes on the micro- to millisecond timescale. These long lifetimes facilitate 'time-gated' emission experiments which result in drastic improvement in signal to noise ratios compared with more traditional steady-state measurements by removing short lived (eg. protein) emission and scattered excitation.

Unfortunately, as consequence of the parity forbidden nature of the 4f transitions, the direct absorption of Ln(III) cations is only very weak, and they hence have very low molar absorption coefficients which limits their practical usage. In order to circumvent these low extinction coefficients, the luminescent metal ion can be chelated to a chromophore-containing group which functions as an 'antenna,' absorbing incident light then transferring this excitation to the metal ion, which can then deactivate by undergoing its typical luminescent emission. In addition to directing energy to the metal, chelation also serves to exclude solvent molecules from the first coordination sphere, which is essential to avoid quenching of the lanthanide luminescence through non-radiative decay via vibronic coupling to vibrational states of O-H and N-H bonds, and also to provide stable metal complexes.

Aza-aromatic bases are widely used in lanthanide coordination chemistry for improving the kinetic stability and photophysical properties of the complexes [83]. In that case, the nitrogen ligand acts as a chromophore which permits effective sensitisation of the lanthanide-centred luminescence.

Some interest for Ln(III) complex formation with heteroaromatic ligands emerged in recent years for the selective complexation of An(III) over Ln(III) by organic molecules, as it seems to be promising for the partitioning of minor actinides from lanthanides, which remains a difficult task in the reprocessing of nuclear wastes because of the close analogies between the chemical properties of these trivalent ions. Examples of ligands studied in recent years are reported in Figure 26 terpyridine (Terpy) derivatives, BTP-family and tripodal ligands (TPA, TPZA) [83]. Due to the generally low solubility of these compounds in water most studies are carried out in organic solvent or mixtures. Despite this widespread interest, very little is known about

the thermodynamics of complex formation with this class of ligands, for example with respect to amines or crown ethers [80].

In this context, we started the study of complex formation between $Ln^{3+}$ ions and the ligands TPA (tris [(2-pyridyl)methyl] amine) and BTPA (6,6'-bis[bis(2-pyridylmethyl)aminomethyl]-2.2'-bipyridine) lanthanide(II) complex formation due to their potential as extracting agents [84] and as sensitizers for photophysical applications.

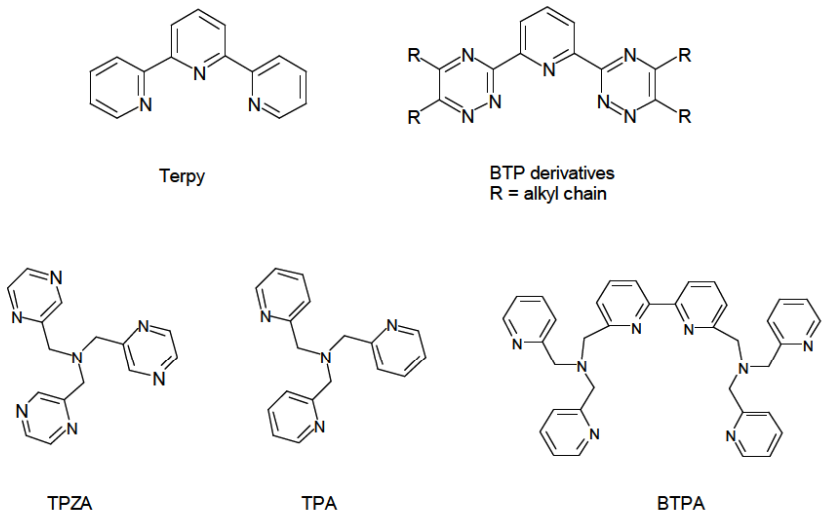


Figure 26 N-donor heteroaromatic ligands potentially interesting for Ln(III) extraction and/or as sensitizers for luminescence applications.

## 3.2. Experimental

### *3.2.1. Chemicals*

Adducts of lanthanide triflate $Ln(CF_3SO_3)_3$ were purchased from Sigma Aldrich and dried under vacuum at 90 °C for 2 weeks in presence of $P_2O_5$. TPA was prepared according to the described procedure [85]. The BTPA ligand [86] has been received from prof. A. Døssing of Copenhagen University. Acetonitrile (Sigma-Aldrich >99%) ware purified by distillation and stored in glove box in presence of molecular sieves [54]. Triflate stock solutions of $Ln^{3+}$ (Ln = La, Pr, Nd, Eu, Gd, Tb, Ho, Er, Tm, Yb and Lu) ions and BTPA ligand were prepared by dissolving in anhydrous degassed AN and stored in a glove box under rigorously anhydrous conditions (see section 2.1.2.1).

Only the heavy (Dy-Lu) lanthanide triflates are soluble (S>150 mM) in strictly anhydrous conditions in AN, while the solubility of the lighter triflates decreases greatly as the atomic weight of the lanthanide decreases [87]. These latter salts are moderately soluble when the water-to-lanthanide(III) concentration ratios are relatively high but their solubilities decrease drastically as water is removed from the solution. We verified that heavier lanthanides have low solubility in AN as only stock solutions of Ln(III) triflates with concentrations $0.8 < C_{Ln} < 2.5$ mM for La-Nd.

### *3.2.2. Absorption spectrophotometry*

The stability constant for the complexes formed between $Ln^{3+}$ ion and BTPA were determined UV-VIS by titrations. Due to the high molar absorption coefficient ($\varepsilon_{290}$ = 15303 $dm^3 \cdot mol^{-1} \cdot cm^{-1}$, $\varepsilon_{268}$ = 1528 $dm^3 \cdot mol^{-1} \cdot cm^{-1}$) (Figure 27) we worked at BTPA concentrations <0.05 mM. In addition, at these concentrations, lanthanide triflates are surely completely dissociated as reported in ref [88].

The electronic spectra were recorded with a Varian Cary 50 Spectrophotometer directly inside the glove box using optic fiber probes and a quartz cuvette with a pathlength of 1 cm.

In a typical experiment, a total of 1 mL of $Ln^{3+}$ solution (additions of 0.1 or 0.05 mL) is added to 2.5 mL of BTPA solution. The ligand BTPA ($2.5 \cdot 10^{-5}$ M < $C_{BTPA}$ < $5.0 \cdot 10^{-5}$ M) has been titrated with $Ln^{3+}$ solution at least twice. The spectral range 250-400 nm has been recorded after each addition with a scan rate 120 nm/min and data interval of 2 nm. The stability constants calculations were performed using the program HypSpec. [56]

A preliminary test where TPA ligand (0.1 mM) was titrated with a solution of $Lu^{3+}$ ion (2 mM) showed that there is no significant change in the initial spectrum. Therefore, we concluded that at these low concentrations the complex is not sufficiently stable to be formed in a significative amount. Further work is in progress on this topic.

## 3.3. Results and discussion

In order to study the formation of complexes between Ln(III) ions and a N-donor ligand like BTPA or TPA in AN it is necessary to work in strict anhydrous conditions. They, in fact, are preferentially solvated by water even in AN containing small quantities of water [87]. The presence of water is less problematic in other aprotic solvents like DMSO or DMF (N,N-dimethylformamide), but preliminary experiments showed that no complex formation occurs in these media. Evidently, Ln(III) ions are strongly solvated and the formation of a stable species does not occur at the accessible experimental conditions (due to the solubility of the ligand). This strong solvent effect can be well understood if the equilibrium in eq. (2.16) is considered: if the solvent molecules are tightly bound to the metal ion, the N-donor ligand is not able to compete with them for the coordination sites.

In anhydrous AN, it has been demonstrated that $Ln(trif)_3$ salts are completely dissociated at concentrations lower than $5\cdot10^{-5}$ M [88]. For this reason, the titration for each lanthanide has been carried out at the lowest Ln(II) concentration possible and avoiding the presence of undissociated salt in solution. This concentration range is however optimal for spectrophotometric titrations as the spectra of BTPA and of its complexes is quite high (Figure 27). In addition, to avoid ion association, no ionic medium was used.

As an example in Figure 28 are reported the spectral changes relative to the titration of BTPA ($3.5\cdot10^{-5}$ M) with $Nd^{3+}$ ($1.6\cdot10^{-4}$ M). The absorption spectrum of BTPA consists of several bands, the maximum at 290 nm is attributed to the bipyridine chromophore and those at 262 and 268 nm to pyridine chromophores [89]. As the titration progresses, increasing the concentration of lanthanide, and therefore the amount of complex formed, a new band appears at higher wavelengths (with a maximum at 320 nm).

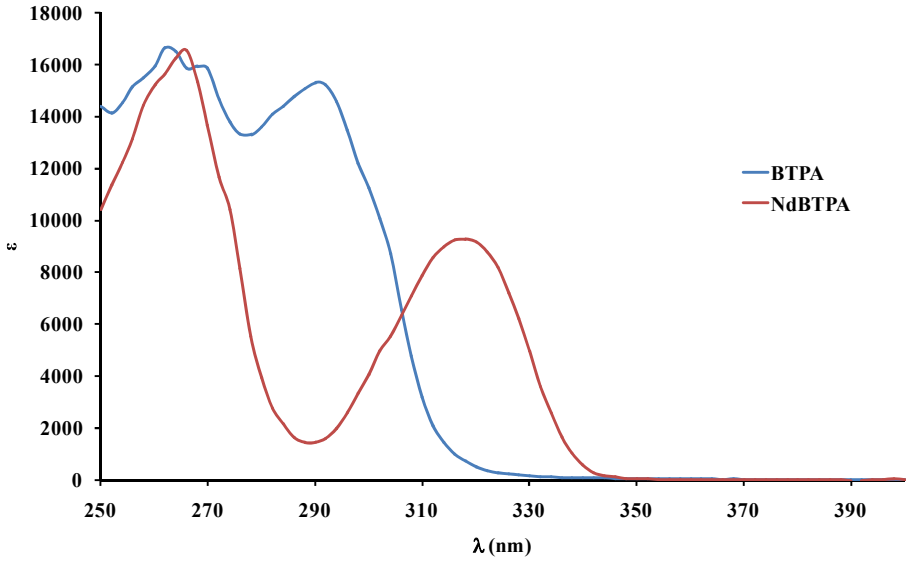


Figure 27 Molar absorption coefficient spectrum of BTPA and $NdBTPA^{3+}$.

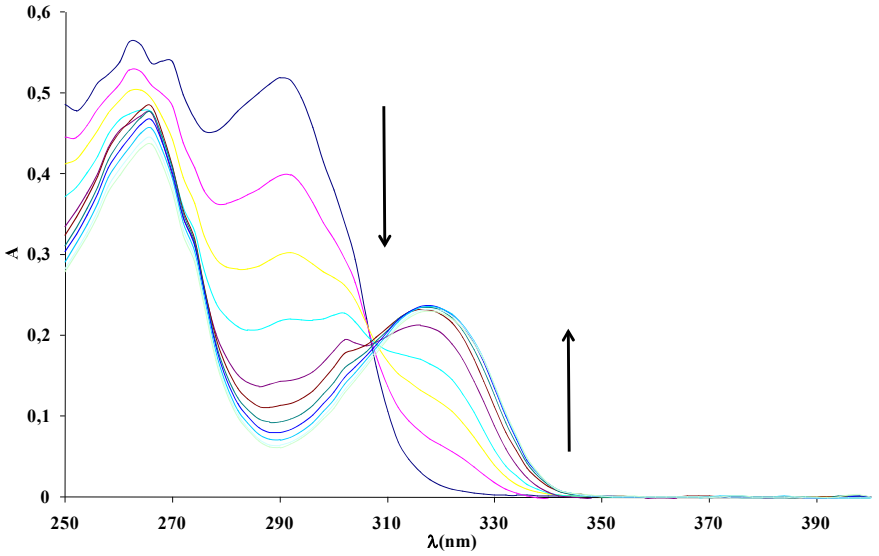


Figure 28 Example of titration of BTPA solution [$3.5 \cdot 10^{-5}$ M] with Nd(III) triflate solution [$1.6 \cdot 10^{-4}$ M] in AN.

The logβ values obtained by the minimization of spectroscopic data in the range 282-332 nm are represented in Figure 29. All values lie in a narrow range (6-7), for this reason, the data are represented, in a fairly large scale, in addition, in this graphic are reported the values of logβ with the error bar corresponding to 1σ. Figure 29 show that nevertheless there is a "W" pattern of the logβ values when plotted against the inverse of the ionic radius ($r^{-1}$) of the Ln(III) ions. The values of logβ decrease from La to a minimum for Nd, then increase until Gd. In the second part of the graph logβ values decrease for Tb and keep constant to increase again for Lu. This stability variation is rather small (maximum distance between two values is 0.73 log units) and seems to be due to a subtle interplay between steric factors, ionic radius and charge density of the lanthanide ion and coordination number.

Additional luminescence experiments for Eu and Tb complexes (visible emission) and Nd, Er and Yb (Near Infrared emission) are ongoing in collaboration with the University of Copenhagen.

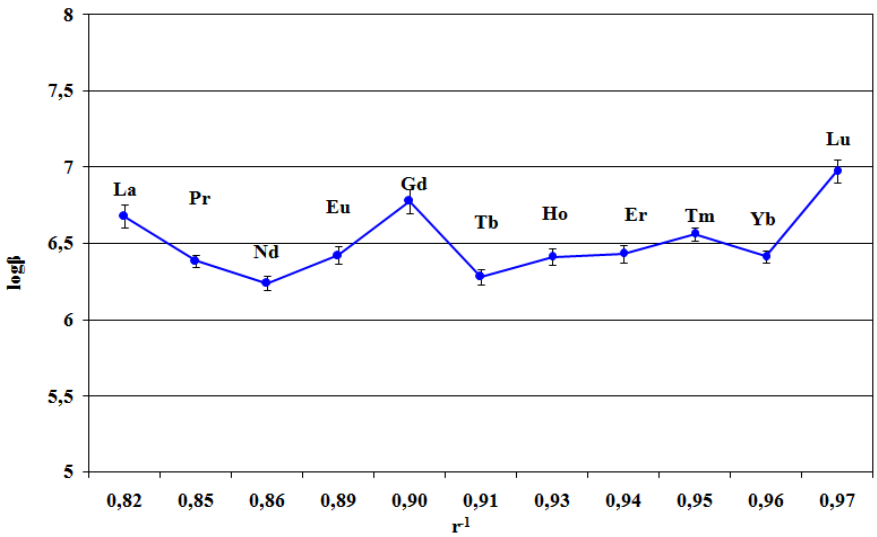


Figure 29 Pot of logb vs. $r^{-1}$ of titration BTPA solution [$3.5 \cdot 10^{-5}$ M] with of Nd(III) triflate solution [$1.6 \cdot 10^{-4}$ M] in AN.

Table 12 Logβ and standard deviations values for the $LnBTPA^{3+}$ complex in AN

| Ln(III) | logβ | 1$\sigma$ |
|---|---|---|
| **La** | 6.68 | 0.08 |
| **Pr** | 6.38 | 0.04 |
| **Nd** | 6.24 | 0.05 |
| **Eu** | 6.42 | 0.06 |
| **Gd** | 6.78 | 0.08 |
| **Tb** | 6.28 | 0.05 |
| **Ho** | 6.41 | 0.05 |
| **Er** | 6.43 | 0.06 |
| **Tm** | 6.56 | 0.04 |
| **Yb** | 6.41 | 0.04 |
| **Lu** | 6.97 | 0.07 |

# 4. Conclusions

Considering the objectives stated in section 1.3 of this thesis and the studies carried out, the results obtained are a contribution to the comprehension of thermodynamics of complexation of metal cations relevant for extraction and pre-concentration processes.

First, a thermodynamic study of complex formation between a set of linear and cyclic thioethers with heavy metals (Ag(II), Zn(II), Cd(II) and Hg(II) has been carried out. The results of these studies indicate that:

- ✓ The linear and cyclic thioethers give strong soft-soft interaction with Hg(II) resulting in highly enthalpy stabilized complexes in AN. A marked selectivity with respect to the soft ion Ag(I) ion is found. With respect to Zn(II) and Cd(II), only formation complex with 9AneS3 and 12AneS4 has been observed, being always much less stable than those formed with Hg(II) and Ag(I).

- ✓ The polarographic measurements show the formation of complexes (1:1) between the mercury and all ligands, except 9AneS3, which is observed in complex formation (1:2) under the conditions of the work.

- ✓ In DMSO the stability of the complexes formed by the two metal ions are closer and more exothermic for Ag(I). In any case a decrease in stability is observed with respect to AN. In addition, no formation of complexes with Zn(II) and Cd(II) is observed.

- ✓ Theoretical calculations show that the high selectivity of 9AneS3 for Hg(II) in AN is originated by a combined coordination/solvation energetics rather than by an intrinsic higher affinity of Hg(II) for 9AneS3. Also the effects of different solvation media, AN and DMSO, are correctly reproduced.

Secondly, the Hg(II)-9AneS3 complexes have been characterized by liquid-liquid distribution processed. In addition, application of the related results to analytical determinations have been carried out by pre-concentration experiments via adsorption sponge supports. The main results were:

- ✓ Preliminary studies of the parameters that affect the extraction processes summarize the following conclusions:

    - No transfer of Hg(II) is observed to organic phase when using 9Anes3 as extractant, rather the formation of metal complexes in aqueous solution is found;
    - The optimum pH range for complex formation is between 0.5 to 3.
    - The temperature does not affect these liquid-liquid processes.
    - The experiments by varying of Hg concentrations and 9AneS3 have shown that total Hg(II) complex formation occurs when the ratio $C_L/C_M$ is equal or over 2, indicating the preferent complex stoichiometry Hg:9AneS3 of 1:2.

- ✓ On the other hand, these studies have shown that complex formation occurs in the aqueous phase. This is important information that has allowed to determine the formation constants of Hg-9AneS3 complexes in water, observing a preferent 1:2 complex and, in less extent the complex 1:3.

- ✓ The values obtained for the formation constants of Hg-9AneS3 complexes by the liquid-liquid distribution studies correlate with those obtained by other techniques used in the present thesis.

- ✓ The use of cellulose common sponge as adsorbent support, impregnated with a solution of the 9AneS3 in hexane, highly increases the pre-concentration of mercury with respect to the untreated sponge. In addition, it has been shown

that for Hg(II) pre-concentration, common cellulose sponge is more efficient than the polyurethane sponge.

Finally, the study regarding to the formation of complexes between lanthanides and BTPA indicate that:

- ✓ The preliminary studies for the determination of formation constants of lanthanide-complex BTPA by UV-Vis spectroscopy show that all lanthanides present a narrow $\log\beta_1$ range (6-7), indicating a poor selectivity for different lanthanides. However, $\log\beta_1$ values present an interesting "W" shaped trend which is likely due to a subtle interplay of steric, solvational and electronic factors.

# Bibliography


1. P. Holmes, K. A. F. James, L. S. Levy, Sci. Total Environ., 408 (2009) 171-182.

2. G. J. Grant, M. E. Botros, J. S. Hassler, D. E. Janzen, C. A. Grapperhaus, M. G. O'Toole, D. G. Vanderveer, Polyhedron, 27 (2008) 3097-3104.

3. M. L. Helm, C. M. Combs, D. G. Vanderveer, G. J. Grant, Inorg. Chim. Acta, 338 (2002) 182-188.

4. V. Mah, F. Jalilehvand, J. Biol. Inorg. Chem., 13 (2008) 541-553.

5. F. M. Rubino, M. Pitton, G. Brambilla, A. Colombi, J. Mass. Spectrom., 41 (2006) 1578-1593.

6. G. A. Neville, T. Drakenberg, Can. J. Chem., 52 (1974) 616-622.

7. V. Mah, F. Jalilehvand, J. Biol. Inorg. Chem., 15 (2010) 441-458.

8. A. Hartwig, M. Asmuss, H. Blessing, S. Hoffmann, G. Jahnke, S. Khandelwal, A. Pelzer, A. Burkle, Food. Chem. Toxicol., 40 (2002) 1179-1184.

9. M. M. Brzoska, J. Moniuszko-Jakoniuk, Food. Chem. Toxicol., 39 (2001) 967-980.

10. C. A. Blindauer, J. Biol. Inorg. Chem., 16 (2011) 1011-1024.

11. W. E. Rauser, Annu. Rev. Biochem., 59 (1990) 61-86.

12. M. J. Stillman, Coordin. Chem. Rev., 144 (1995) 461-511.

13. M. Shamsipur, M. H. Mashhadizadeh, Sep. Purif. Technol., 20 (2000) 147-153.

14. M. Shamsipur, O. R. Hashemi, V. Lippolis, J. Mater. Sci., 282 (2006) 322-327.

15. J. R. Morones, J. L. Elechiguerra, A. Camacho, K. Holt, J. B. Kouri, J. T. Ramirez, M. J. Yacaman, Nanotechnology, 16 (2005) 2346-2353.

16. Z. J. Jiang, C. Y. Liu, L. W. Sun, J. Phys. Chem. B, 109 (2005) 1730-1735.

17. A. Bianchini, K. C. Bowles, C. J. Brauner, J. W. Gorsuch, J. R. Kramer, C. M. Wood, Environ. Toxicol. Chem., 21 (2002) 1294-1300.

18. P. L. Drake, K. J. Hazelwood, Ann. Occup. Hyg., 49 (2005) 575-585.

19. P. Nagajyoti, K. Lee, T. Sreekanth, V, Environ. Chem. Lett., 8 (2010) 199-216.

20. X. Li, R. Z. Liao, W. Zhou, G. Chen, Phys. Chem. Chem. Phys., 12 (2010) 3961-3971.

21. M. Belcastro, T. Marino, N. Russo, M. Toscano, J. Inorg. Biochem., 103 (2009) 50-57.

22. M. Belcastro, T. Marino, N. Russo, M. Toscano, J. Mass. Spectrom., 40 (2005) 300-306.

23. S. P. Fricker, Chem. Soc. Rev., 35 (2006) 524-533.

24. P. Babula, V. Adam, R. Opatrilova, J. Zehnalek, L. Havel, R. Kizek, Environ. Chem. Lett., 6 (2008) 189-213.

25. H. Ilkhani, M. R. Ganjali, M. Arvand, M. S. Hejazi, F. Azimi, P. Norouzi, Int. J. Biol. Macromol., 49 (2011) 1117-1123.

26. J. Rocha, L. D. Carlos, F. A. Almeida Paz, D. Ananias, Chem. Soc. Rev., 40 (2011) 926-940.

27. J. F. Carpentier, S. M. Guillaume, E. Kirillov, Y. Sarazin, C. R. Chim., 13 (2010) 608-625.

28. S. A. El-Safty, J. Mater. Sci., 44 (2009) 6764-6774.

29. D. M. Roundhill, Extraction of metals from soils and waters, Kluwer Academic/Plenum Publishers, United States, 2001.

30. K. Saito, I. Taninaka, Y. Yamamoto, S. Murakami, A. Muromatsu, Talanta, 51 (2000) 913-919.

31. A. Nezhadali, N. Rabani, Chinese Chem. Lett., 22 (2011) 88-92.

32. A. L. Ahmad, A. Kusumastuti, C. J. C. Derek, B. S. Ooi, Chem. Eng. J., 171 (2011) 870-882.

33. M. Shamsipur, G. Azimi, M. H. Mashhadizadeh, S. S. Madaeni, Anal. Sci., 17 (2001) 491-494.

34. P. K. Mohapatra, D. S. Lakshmi, D. Mohan, V. K. Manchanda, J. Mater. Sci., 232 (2004) 133-139.

35. N. S. Rathore, J. V. Sonawane, A. Kumar, A. K. Venugopalan, R. K. Singh, D. D. Bajpai, J. P. Shukla, J. Mater. Sci., 189 (2001) 119-128.

36. R. Gueell, E. Antico, V. Salvado, C. Fontas, Sep. Purif. Technol., 62 (2008) 389-393.

37. R. G. Pearson, J. Am. Chem. Soc., 85 (1963) 3533-3539.

38. R. G. Parr, R. G. Pearson, J. Am. Chem. Soc., 105 (1983) 7512-7516.

39. Msrtell A. E., Hancock R. D., Metal Complexes in Aqueous Solutions. 1996, Plenum Press, New York.

40. M. L. Helm, L. L. Hill, J. P. Lee, D. G. Van Derveer, G. J. Grant, Dalton Trans., (2006) 3534-3543.

41. M. L. Helm, G. P. Helton, D. G. Vanderveer, G. J. Grant, Inorg. Chem., 44 (2005) 5696-5705.

42. F. J. C. Rossotti, H. Rossotti, The determination of stability constants: and other equilibrium constants in solution, McGraw-Hill, USA, 1961.

43. P. Atkins, J. D. Paula, Atkins' Physical Chemistry, W H Freeman & Co, United States, 2006.

44. Y. Marcus, The properties of solvents, John Wiley and Sons Australia, United Kingdom, 1998.

45. P. Di Bernardo, A. Melchior, R. Portanova, M. Tolazzi, P. L. Zanonato, Coordin. Chem. Rev., 252 (2008) 1270-1285.

46. G. J. Grant, Structure and Bonding, 120 (2006) 107-141.

47. F. Baumann, G. Reynolds, Chem. Commun., (1998) 1637-1638.

48. M. Mameli, V. Lippolis, C. Caltagirone, J. Luis Capelo, O. Nieto Faza, C. Lodeiro, Inorg. Chem., 49 (2010) 8276-8286.

49. M. L. Helm, D. G. Vanderveer, G. J. Grant, J. Chem. Crystallogr., 33 (2003) 625-630.

50. J. Ishikawa, H. Sakamoto, M. Nakamura, K. Doi, H. Wada, J. Chem. Soc. , Dalton Trans., (1999) 191-199.

51. M. R. Ganjali, A. Rouhollahi, A. R. Mardan, M. Shamsipur, J. Chem. Soc. , Faraday Trans., 94 (1998) 1959-1962.

52. R. Alberto, W. Nef, A. Smith, T. A. Kaden, M. Neuburger, M. Zehnder, A. Frey, U. Abram, P. A. Schubiger, Inorg. Chem., 35 (1996) 3420-3427.

53. C. Comuzzi, M. Grespan, A. Melchior, R. Portanova, M. Tolazzi, Eur. J. Inorg. Chem., (2001) 3087-3094.

54. A. Cassol, P. Di Bernardo, P. Zanonato, R. Portanova, M. Tolazzi, J. Chem. Soc. , Dalton Trans., (1987) 657-659.

55. A. I. Vogel, G. H. Jeffery, Vogel's textbook of quantitative chemical analysis, Longman Scientific & Technical, England, 1989.

56. P. Gans, A. Sabatini, A. Vacca, Talanta, 43 (1996) 1739-1753.

57. J. O. Hill, G. Öjelund, I. Wadsö, J. Chem. Thermodyn., 1 (1969) 111-116.

58. P. Gans, A. Sabatini, A. Vacca, J. Solution Chem., 37 (2008) 467-476.

59. J.Heyrovsky, J.Kuta, Polarography, Academic Press, New York 1966.

60. A. I. Vedernikov, E. N. Ushakov, L. G. Kuz'mina, A. V. Churakov, Y. A. Strelenko, M. Wörner, A. M. Braun, J. A. K. Howard, M. V. Alfimov, S. P. Gromov, J. Phys. Org. Chem., 23 (2010) 195-206.

61. R. P. Zelinski, B. W. Turnquest, E. C. Martin, J. Am. Chem. Soc., 73 (1951) 5521-5523.

62. D. A. Rappoport, W. Z. Hassid, J. Am. Chem. Soc., 73 (1951) 5524-5525.

63. M. J. Frisch, G. W. Trucks, H. B. Schlegel et al., GAUSSIAN 09, Revision A.1, Gaussian, Inc., Wallingford, CT, 2009.

64. S. Ahrland, Pure Appl. Chem., 62 (1990) 2077-2082.

65. O. Akkus, A. Decken, C. Knapp, J. Passmore, J. Chem. Crystallogr., 36 (2006) 321-329.

66. Y. Tsutsui, K. Sugimoto, H. Wasada, Y. Inada, S. Funahashi, J. Phys. Chem. A, 101 (1997) 2900-2905.

67. D. M. Roundhill, I. B. Solangi, S. Memon, M. I. Bhanger, M. Yilmaz, Pak. J. Anal. Environ. Chem., 10 (2009) 1-13.

68. F. Fu, Q. Wang, J. Environ. Manag., 92 (2011) 407-418.

69. T. F. Baumann, J. G. Reynolds, G. A. Fox, React. Funct. Polym., 44 (2000) 111-120.

70. C. A. Sharrad, L. Grondahl, L. R. Gahan, J. Chem. Soc. , Dalton Trans., (2001) 2937-2942.

71. T. Suzuki, D. Tiwari, A. Hioki, Anal. Sci., 23 (2007) 1215-1220.

72. Manual VGPQ Excell Traning Manual, 1998. ThermoOptek, Windsford, UK

73. F. Vanhaecke, H. Vanhoe, R. Dams, C. Vandecasteele, Talanta, 39 (1992) 737-742.

74. Manual. Innov-X systems Alpha seriesTM X-Ray fluorescence spectrometers, Innov-X Systems Inc., Woburn, MA, USA, 2005.

75. D. A. Skoog, J. J. Leary, C. A. Blasco, Anáílisis instrumental, McGraw-Hill, 1994.

76. Arnold Klute, Methods of soil analysis, Part 1: Physical and microbiological properties, Agronomy Serie nº9, USA, 1986.

77. C. Fontes, C. Palet, V. Salvador, M. Hidalgo, J. Mater. Sci., 178 (2000) 131-139.

78. M. Oleinikova, C. González, M. Valiente, M. Muñoz, Polyhedron, 18 (1999) 3353-3359.

79. D.H. Liem, Acta Chem. Sacand, 25, 1521 (1971)

80. P. Di Bernardo, A. Melchior, M. Tolazzi, P. L. Zanonato, Coordin. Chem. Rev., 256 (2012) 328-351.

81. A. Braibanti, V. Carunchio, I complessi metallici in soluzione. Reattività ed equilibri, metodologie, applicazioni, Aracne, 1999.

82. D. Parker, R. S. Dickins, H. Puschmann, C. Crossland, J. A. K. Howard, Chem. Rev., 102 (2002) 1977-2010.

83. G. Ionova, C. Rabbe, R. Guillaumont, S. Ionov, C. Madic, J. C. Krupa, D. Guillaneux, New J. Chem., 26 (2002) 234-242.

84. R. Wietzke, M. Mazzanti, J. M. Latour, J. Pecaut, P. Y. Cordier, C. Madic, Inorg. Chem., 37 (1998) 6690-6697.

85. G. Anderegg, F. Wenk, Helv. Chim. Acta, 50 (1967) 2330-2332.

86. A. Dossing, A. Hazell, H. Toftlund, Acta. Chem. Scand., 50 (1996) 95-101.

87. P. Di Bernardo, G. R. Choppin, R. Portanova, P. L. Zanonato, Inorg. Chim. Acta, 207 (1993) 85-91.

88. A. F. D. de Namor, S. Chahine, O. Jafou, K. Baron, J. Coord. Chem., 56 (2003) 1245-1255.

89. A. Dossing, H. Toftlund, A. Hazell, J. Bourassa, P. C. Ford, J. Chem. Soc. , Dalton Trans., (1997) 335-339.